

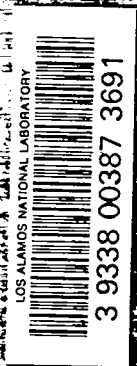
LA-4546-MS

C.3

CIC-14 REPORT COLLECTION  
REPRODUCTION  
COPY

LOS ALAMOS SCIENTIFIC LABORATORY  
of the  
University of California  
LOS ALAMOS • NEW MEXICO

Quarterly Status Report on the  
Advanced Plutonium Fuels Program  
July 1-September 30, 1970



UNITED STATES  
ATOMIC ENERGY COMMISSION  
CONTRACT W-7405-ENG 36

This report was prepared as an account of work sponsored by the United States Government. Neither the United States nor the United States Atomic Energy Commission, nor any of their employees, nor any of their contractors, subcontractors, or their employees, makes any warranty, express or implied, or assumes any legal liability or responsibility for the accuracy, completeness or usefulness of any information, apparatus, product or process disclosed, or represents that its use would not infringe privately owned rights.

This LA...MS report presents the status of the LASL Advanced Plutonium Fuels Program. Previous Quarterly Status Reports in this series, all unclassified, are:

LA-3607-MS	LA-3820-MS	LA-4193-MS
LA-3650-MS	LA-3880-MS	LA-4284-MS
LA-3686-MS	LA-3933-MS	LA-4307-MS
LA-3708-MS*	LA-3993-MS	LA-4376-MS
LA-3745-MS	LA-4073-MS	LA-4437-MS
LA-3760-MS*	LA-4114-MS	LA-4494-MS

This report, like other special-purpose documents in the LA...MS series, has not been reviewed or verified for accuracy in the interest of prompt distribution.

\*Advanced Reactor Technology (ART) series.

Distributed: November 1970

LA-4546-MS  
SPECIAL DISTRIBUTION

**LOS ALAMOS SCIENTIFIC LABORATORY**  
of the  
**University of California**  
LOS ALAMOS • NEW MEXICO

Quarterly Status Report on the  
**Advanced Plutonium Fuels Program**  
July 1-September 30, 1970



## FOREWORD

This is the 17th quarterly report on the Advanced Plutonium Fuels Program at the Los Alamos Scientific Laboratory.

Most of the investigations discussed here are of the continuing type. Results and conclusions described may therefore be changed or augmented as the work continues. Published reference to results cited in this report should not be made without obtaining explicit permission to do so from the person in charge of the work.

## CONTENTS

<u>PROJECT</u>		<u>PAGE</u>
401	EXAMINATION OF FAST REACTOR FUELS	1
	I. Introduction	1
	II. Equipment Development	1
	III. Hot Cell Facility at DP West	3
	IV. Methods of Analysis	4
	V. Requests from DRDT	6
	VI. References	7
463	CERAMIC PLUTONIUM FUEL MATERIALS	8
	I. Introduction	8
	II. Synthesis and Fabrication	8
	III. Irradiation Testing	9
	IV. Properties	10
	V. Publications	20
	VI. References	20
472	ANALYTICAL STANDARDS FOR FAST BREEDER REACTOR OXIDE FUEL	22
	I. Introduction	22
	II. FFTF Analytical Chemistry Program	22
	III. Investigation of Methods	23
	IV. References	28

PROJECT 401  
EXAMINATION OF FAST REACTOR FUELS

Person in Charge: R. D. Baker  
Principal Investigators: J. W. Schulte  
J. A. Leary  
C. F. Metz

---

I. INTRODUCTION

This project is directed toward the examination and comparison of the effects of neutron irradiation on LMFBR Program fuel materials. Unirradiated and irradiated materials will be examined as requested by the Fuels and Materials Branch of DRDT. Capabilities are established for providing conventional pre-irradiation and post-irradiation examinations. Additional capabilities include less conventional properties measurements which are needed to provide a sound basis for steady-state operation of fast reactor fuel elements, and for safety analysis under transient conditions.

Analytical chemistry methods that have been modified and mechanized for hot cell manipulators will continue to be applied to the characterization of irradiated fuels. The shielded electron microprobe and emission spectrographic facilities will be used in macro and micro examinations of various fuels and clads. In addition, new capabilities will be developed with emphasis on gamma scanning and analyses to assess spatial distribution of fuel and fission products.

High temperature properties of unirradiated LMFBR fuel materials are now being determined by Contractor in an associated project (ident No. 07463). Equipment designs and interpretive experience gained in this project are being extended to provide unique capabilities such as differential thermal analysis, melting point determination, high temperature dilatometry, and high temperature heat content and heat of fusion for use on irradiated materials.

II. EQUIPMENT DEVELOPMENT

A. Inert Atmosphere Systems  
(C. E. Frantz, P. A. Mason, R. F. Velkinburg)

1. Disassembly Cell. The Ar recirculating purifier used for the disassembly cell has been successfully demonstrated over a period of several consecutive weeks. During this time the O<sub>2</sub> and H<sub>2</sub>O concentrations of the box atmosphere were typically 20 ppm and 5 ppm, respectively. Leaks in a manipulator boot developed, and it was necessary to revert to the purge type of operation. Consequently, the purifier has been used only on an intermittent basis.

Since the primary source of leaks in this system continues to be the manipulator booting, it is hoped that the use of sealed-type manipulators, such as the Model L units recently received, will be effective in minimizing the in-leakage of air.

2. Metallography Cells. The partially damaged oxygen absorbent bed in the recirculating Ar purifier was replaced with Girdler Catalyst produced by Chemetron Corporation. Upon placing the purifier in service, air in-leakage was excessive, and the purifier was shut down. Extensive leak checking and a study of the system indicates that there are major leaks below the alpha boxes and within the cell shielding. Access to these areas will be possible in October at which time the leaks will be located and corrected.

The once-through Ar purge system for the metallography cells provides atmospheres containing 1000 to 3000 ppm O<sub>2</sub> and about 10 ppm H<sub>2</sub>O.

B. Heat Content Measurement  
(G. R. Brewer, C. E. Frantz)

Work was continued during this period in preparing to obtain measurements on irradiated oxide fuel for comparison with the results obtained on unirradiated specimens.

About 45 g of irradiated (U, Pu)O<sub>2</sub> was encapsulated in tungsten using the remotized welder. It was necessary to open this capsule to retrieve a small sample. This was successfully accomplished by carefully breaking off the capsule lid. The fuel did not appear to be contaminated with tungsten as a result of this operation.

A portion of the calorimeter piping was changed to permit running the calorimeter under an Ar atmosphere. A series of electrical calibrations was completed on the calorimeter using an Ar atmosphere. The method of Jessup<sup>1</sup> was used in reducing the data. High temperature operations of the furnace under an Ar atmosphere have not yet been attempted.

Since the equipment has now been installed and tested, this phase of the work has been completed. A report describing the conversion of a drop calorimeter design to use on irradiated materials in a shielded environment is being prepared.

The results obtained using this equipment will hereafter be contained in the "Properties" section of Project 463.

C. Thermal Diffusivity  
(M. E. Lazarus, J. M. Ledbetter,  
R. F. Velkinburg)

The high temperature vacuum furnace, ordered for thermal diffusivity measurements on irradiated Pu bearing fuels, has been received. The furnace and associated equipment have been assembled for testing, and a few problems were discovered. The company will have a representative at LASL in October to check and repair the system.

D. In-Cell Equipment  
(E. L. Ekberg, F. J. Fitzgibbon, C. D. Montgomery, P. P. Osvath, T. Romanik,  
J. R. Trujillo, R. F. Velkinburg)

1. Element-Sectioning Saw. The components for the modified "Econo-Saw" have been received and assembled. Installation of the saw in the disassembly cell is expected to be made in the near future. It is hoped that this unit will not only provide more flexibility in sawing a variety of fuels and materials, but also will produce less dust than is encountered with the high speed abrasive saw currently being used.

2. Microsampling Apparatus. A commercially available remote positioner having an accuracy of 0.0005 in. has been located and checked for compatibility with the overall design requirements of the microsampling equipment. This item will be ordered for incorporation into this system in the near future.

3. CRL Type L Sealed Manipulators. Two Model "L" sealed manipulators were received from Central Research Laboratories. The units were assembled, adjusted, and functionally checked out and are now awaiting completion of adapter wall tubes. These manipulators were purchased to provide more control over the atmosphere purity in the alpha containment boxes. A series of tests is planned to check the suitability of these units for this purpose. If successful, the manipulator boots would be required to serve only one function, that of protecting the manipulators from being contaminated.

E. New Metallograph Installation  
(C. D. Montgomery, T. Romanik)

A revised "blister" is needed to accommodate the new metallograph and accessory equipment which will be located adjacent to the polishing cell. This unit which will replace the present "blister" is tentatively scheduled to contain the following pieces of equipment.

1. The existing B and L metallograph
2. A new commercially remotized Leitz metallograph.
3. An etching station
4. A Quantimet image analyzer

The Leitz metallograph has been received and is being incorporated into the overall design. The Quantimet image analyzer is on order for delivery in October. The etching components are on order. One of the mini-manipulators is now on hand; the other unit was returned to the vendor to correct the damage which occurred in shipment.

F. Scanning Electron Microscopy  
(K. A. Johnson)

The basic operating unit has arrived, and assembly by factory personnel will start after October 20, at which time it is estimated that the necessary services will be installed.

G. Miscellaneous  
(C. E. Frantz, M. E. Lazarus, J. M. Ledbetter,  
P. A. Mason, C. D. Montgomery)

The low flow rate of Ar used with either the recirculating purification systems or the purge method is not sufficient to carry off the heat produced in the alpha box by the mercury vapor lamps. Consequently, tests have been run which indicate that cooling water circulated through coils, silver soldered to the top of the box, has been effective in reducing the temperature (near the top of the box) from 116° F to 83° F. Since it is desirable to maintain the box near room temperature to extend the life of manipulator boots, motors, and other in-cell equipment, additional tests may be run to determine optimum conditions of operation.

Inert Atmospheres for Transfer Containers. A new station for providing inert atmospheres in transfer containers is being designed. The atmosphere of the containers will be rendered inert by either evacuating and backfilling with Ar, or by purging with Ar.

Several transfer cans, 7 in. diam, are being modified by the addition of a small check valve to the lid of the can. This change will permit use of the existing station with the evacuation and back-fill method for providing inert atmosphere.

Sodium Distillation Apparatus. Preliminary designs are in progress to improve the apparatus in the disassembly cell for removing Na from sections of fuel pins by distillation. It is planned that the new device will provide a better vacuum and a higher temperature for the system. The cold trap used for condensing the Na and radioactive I<sub>2</sub> will be designed to be remotely cleaned and replaced.

Shipping Cask. The design of the new cask for shipping small sections of fuel pins and other irradiated materials is currently being reviewed. The cask was designed to meet the current DOT regulations required for transporting radioactive materials.

Immersion Densities on Cladding. The sensitivity of the in-cell equipment was found to be adequate for determining density changes in cladding materials exposed to fast neutron irradiation.

III. HOT CELL FACILITY AT DP WEST  
(F. J. Fitzgibbon, M. E. Lazarus, J. R. Phillips,  
C. D. Montgomery, J. R. Trujillo)

The current status of the major systems and operations at the modified DP West Hot Cell Facility are listed below.

A. Structures and Equipment

1. Drilling of all holes in the high density concrete cells has been completed.
  2. The 25-ton hoist structure was completed; the hoist was installed and checked out. Installation of electrical wiring is in progress.
  3. The 3-ton corridor crane has been installed, and a modification is in process to change the present building stops to permit additional travel in the north direction.
  4. The 1/2-ton hoist in the operating area has been installed and will permit handling of manipulators, periscopes, and other items in that area.
  5. The 23-ton capacity cart for moving casks between the hot cell corridor and the unloading station under the 25-ton hoist has been completed, delivered, and satisfactorily checked out under load.
  6. The 6000-lb capacity forklift for moving the cask cart and shielded casks has been received and tested.
  7. The adapters for removing storage inserts from the floor holes in the corridor are being fabricated. A prototype unit was received and satisfactorily tested.
  8. Criticality studies are in progress to determine if as many as 25 fast reactor fuel pins can be stored in each of the 4 cells and each of the 22 storage holes at any given time.
- B. Hot Cell Equipment
1. Gamma Scanning System. (a) A special wall liner to accommodate the collimator-adjusting mechanism was fabricated and is ready for installation. (b) The track and support stand for the scanner shield assembly has been fabricated and is presently awaiting an appropriate installation time. (c) The fuel pin handling system for inside the cell has been completed and is in process of being wired. (d) One collimator (0.014-in. hole) has been completed to the point of pouring lead.



This particular collimator utilizes a Au and W primary collimator backed up by Pb. (e) The vendor furnishing the step control drive and read-out system for the pin-handling mechanisms is incorporating some changes to provide compatibility with the existing drive units. The motors and encoders are to be available for testing in October.

2. Profilometer. All in-cell equipment is complete with the exception of electrical wiring. The status of the work area equipment is as follows:

Electro Optical Sensor -- On hand

Sensor Positioning Stand -- Under construction

Data Storage System -- All equipment except Tape Deck and Tape Controller on hand. This system needs assembly and wiring.

3. Macrophotography. Construction of equipment has been completed. Electrical wiring and testing should be finished in October.

#### IV. METHODS OF ANALYSIS

A. Measurement of U and Pu  
(J. W. Dahlby and G. R. Waterbury)

Controlled-potential coulometric equipment, previously modified for titrating U and Pu in the chemical characterization of irradiated mixed oxide or mixed carbide fuels, was applied successfully to the measurement of each metal without chemical separation in a  $(U_{0.8}Pu_{0.2})O_2$  fuel having undergone about 6% burnup. In these measurements, titration techniques were used that had been found to be successful in the reliable analyses of fuels having undergone 1 at.% burnup. The quantity of uranium or plutonium titrated was reduced to less than 1 mg; the sample was fumed with  $H_2SO_4$  immediately before the titration; and redox cycling, for the plutonium titrations, or titration blank corrections, for the uranium measurements, were applied. These techniques eliminated the deleterious effects of radiolytic decomposition products in the aqueous solutions.

Two cross sections of the fuel were dissolved separately, and eight aliquots containing 3 mg of fuel (0.5 mg of Pu) from each solution were analyzed for Pu, and eight aliquots containing 1 mg of fuel (0.6 mg of U) were analyzed for U. For the measurement of Pu, the current for the coulometric oxidation of Pu(III) to Pu(IV)

at a Pt electrode was integrated, and then the current for the coulometric reduction of Pu(IV) to Pu(III) was integrated. The oxidation and reduction cycles were repeated until consecutive values for the Pu differed by less than 2  $\mu$ g. The results for Pu in the two samples were 17.0 and 17.4% (Table 401-II). The precision (1  $\sigma$ ) was 0.1% which was equal to the precision obtained for titrations of the 1% burnup fuels.

TABLE 401-II  
MEASURED U AND Pu CONTENTS OF  $(U, Pu)O_2$  FUELS  
(6 at.% Burnup)

Cross Section	Pu, %	Std. Dev., %	U, %	Std. Dev., %	Total U + Pu, %
1	17.0	0.1	65.3	0.3	82.3
2	17.4	0.1	64.5	0.3	81.9

The integrated current for the coulometric reduction of U(VI) at a Hg electrode to U(IV), following a preliminary reduction of more-easily reduced impurities, was used in calculating the U content. Following each titration, the aliquot was left in the titration cell for a time equal to that required for the original titration, and then the titration was repeated to obtain a blank. This blank was subtracted from the coulombs of electricity used in the original titration to correct for the effect of peroxides generated radiolytically. The results obtained for U were 65.3 and 64.5% (Table 401-II), and the precision (1  $\sigma$ ) was 0.3%, which was in agreement with the precision obtained for samples having undergone only 1% burnup.

The differences between the average results for Pu and U in the two cross sections are significant, but the totals of the U and Pu in the two samples of 82.3 and 81.9% are in good agreement. The average of the totals of U and Pu of 82.1% is 5.9% lower than the original composition of the fuel, indicating a burnup close to the calculated 6%. Additional mixed oxide fuels and  $(U, Pu)C$  fuels, also having undergone 6% burnup, are being analyzed to complete testing of the method for analyzing fuel having this burnup level. Methods to separate U and Pu from most of the fission product activities are being considered.

B. Determination of O<sub>2</sub> in Irradiated Fuels  
(C. S. MacDougall, M. E. Smith,  
G. R. Waterbury)

Testing of an analytical system for measuring O<sub>2</sub> in various irradiated materials was completed by analyzing several samples of U<sub>3</sub>O<sub>8</sub> prepared with a known O<sub>2</sub> content of 15.24% from U metal having less than 100 ppm of total detected impurities. The average of repeated analyses was 15.24%, showing that no bias existed, and the relative standard deviation (1 σ) was 0.2% which was equal to the precision of the method when used outside of the hot cell.

Samples of irradiated, stainless-steel cladding were then analyzed without difficulty. The results ranged between 0.14 and 0.25% O<sub>2</sub>. Analyses of the unirradiated, stainless steels for O<sub>2</sub> were not available for comparison, and the accuracy of the measurements could not be estimated. Remote operation of the equipment proved satisfactory in these analyses.

Samples of irradiated, (U, Pu)O<sub>2</sub> fuels are being prepared for measurement of O<sub>2</sub> at this time.

C. Gamma Scanning  
(J. Phillips)

Gross gamma scanning rapidly provides information about areas of interest for further analyses and destructive sectioning of irradiated fuel elements. Much additional information may be obtained nondestructively by high-resolution gamma scanning which identifies and measures specific isotopes and determines their spatial distributions. The new gamma scanning system (Nuclear Data 50/50) now being assembled and tested for use at the DP West hot cell facility will provide capabilities for gross gamma scanning and either one-dimensional or two-dimensional high-resolution gamma scanning of up to 30 individual isotopes. Various components of the system have been tested individually and in partial assembly, but the complete system cannot be tested until satisfactory stepping motors for the scan-drive mechanism are obtained. Installation of new motors by the vendor is scheduled early next quarter.

Computer codes for the new systems have been developed to the stage that plots of the radial distribution of each fission product element measured can be made

from data obtained with the electronic components of the Nuclear Data 50/50 system and the scanning drive mechanism from the old gamma scanner. Modifications are being made in the computer codes to improve spatial resolution in the plots which now is 0.020 to 0.030 in.

Testing was completed of the detector system which consists of an anticoincidence shield with a NaI annulus and a high efficiency (12.1%) Ge(Li) detector. The results showed that the detector system was satisfactory, but noise in the electronic components adversely affected the resolution. The source of the electronic noise is being sought.

Fabrication of the newly designed collimators was started. The Au insert for the pinhole collimator was made, and casting equipment was set up to fabricate other components.

Every effort is being made to have the gamma scanning system completely assembled and tested by the time the hot cell modifications are finished to avoid delays in the installation at the DP West facility.

D. Dissolution of Metallic Fission Product Alloys  
(J. W. Dahlby, G. C. Swanson, G. R. Waterbury)

Metallic inclusions composed of fission product Mo, Rh, Ru, and Tc have often been found in fuels having undergone several percent burnup. All dissolution methods applied to these inclusions to date reportedly have been ineffective, and as a consequence, accurate analyses of the alloy compositions have not been made chemically. In an effort to solve this difficult problem, two strenuous dissolution methods were tested using alloys made from the four nonradioactive metals for test samples. The alloys were prepared using electric arc melting to have the approximate compositions shown in Table 401-III.

TABLE 401-III

<u>Metal</u>	<u>Composition, w/o</u>	
	<u>Alloy 1</u>	<u>Alloy 2</u>
Mo	44.18	49.80
Rh	14.66	16.68
Ru	39.75	8.33
Tc	1.40	25.18

The first dissolution method tried used an a.-c. electrolytic dissolver at an applied potential of 4 to 5 V

between two vitreous carbon electrodes. One electrode was cup-shaped and held a 50- to 100-mg sample of the alloy in 12M HCl solution originally, but the acid strength decreased to < 0.1M during electrolysis. Repeated tests showed that at least 99% of either alloy was dissolved within 15 h, but the slight amount of residue (< 0.5 mg) was not dissolved by adding fresh 12M HCl and further electrolysis. Spectrographic analysis of the residue showed that it contained the four metals of the original alloy. Additional tests are being made in which the acid, acid strength, applied voltage, and distance between electrodes are being varied in an effort to dissolve the sample completely. Dissolution of 99% of the sample, however, should be adequate for many applications.

In the second dissolution method, 50 to 60 mg of the alloy and 7 ml of 12M HCl containing 3 to 4 drops of 12M HClO<sub>4</sub> were sealed in a fused-silica tube and heated to 300° C. Internal pressures approaching 4000 psi were generated and accelerated the dissolution. Complete dissolution of each alloy was accomplished in about 15 h. Equipment was designed and fabrication was started for a remotely operated dissolution system of this type. The method will be used with fission product alloys when installation in the hot cell is completed.

#### V. REQUESTS FROM DRDT

##### A. Examination of Irradiated Material

(K. A. Johnson, E. D. Loughran (GMX-2),  
R. A. Morris (GMX-1), J. R. Phillips,  
J. W. Schulte, G. R. Waterbury)

Los Alamos Scientific Laboratory. After irradiation of experimental capsule OWREX 15 in Omega West Reactor at LASL, the following were completed: visual inspection, radiation measurements, radiography, gamma scan, Na removal by heat and dissolution, and macrophotography.

Metallographic examinations of the OWREX 14 and 15 specimens listed below included macrophotography, alpha and beta-gamma autoradiography and optical metallography. (Table 401-IV)

Autoradiography, macrophotography, Na removal, sectioning, and metallography were carried out in an Ar atmosphere.

LASL capsules 36-B and 42-B were received on

September 29, and nondestructive tests were started immediately.

TABLE 401-IV  
METALLOGRAPHY OF OWREX TESTS

Element No.	Number of Specimens		
	Stainless Steel Pellets	Fuel	Cladding
OWREX 14	1	1	3
OWREX 15	1	2	3

#### Nuclear Materials and Equipment Corporation.

Specimens were removed from each of the NUMEC B-1, B-9, and B-11 fuel pins for the purpose of making DTA measurements.

Fuel from NUMEC B-9 was encapsulated (as described in Section II. B) in a W container for making heat content measurements.

A W capsule which contained fuel from NUMEC B-9 and which had been exposed to several DTA cycles, was opened and prepared for metallography. This latter study is now in progress.

Cask 5885 is being shipped to NUMEC for the return of 11 irradiated pins from the A Series Experiments.

A shielded microprobe was used to examine samples of NUMEC B-11 pin from those areas where various degrees of failure of cladding had occurred and from an area where the cladding had not failed.

United Nuclear Corporation. Examinations of 22 capsules, pins, or sections of pins were made by performing the tests, measurements, or operations enumerated below.

Examination of UNC-210 through -221 (12 rabbit irradiations) involved items 1 through 5, and item 8 listed below. Capsule UNC-213 was the only unit on which gamma scanning was performed.

Experimental units UNC-125 through -128 were inspected according to the operations listed in items 6 through 10; items 1 through 5 had been examined in the preceding quarter.

1. Visual inspection and photography
2. Measurements of contamination and radiation
3. Measurements of temperature
4. Radiography

5. Micrometer measurements
6. Gamma scanning
7. Profilometry
8. Analyses of cover gas in capsules and fission gas in pins.
9. Sectioning in an Ar atmosphere
10. Measurements of density by immersion were made on fuel fragments from UNC-125 through -128, and clad samples from both the fuel area and the gas plenum area of UNC-81 through -86.

Metallographic examinations, consisting of macro-photography, alpha and beta-gamma autoradiography, and optical metallography, are currently in process on the specimens tabulated in Table 401-V.

TABLE 401-V

METALLOGRAPHY OF UNC SPECIMENS

<u>Element No.</u>	<u>Fuel-Cladding</u>	<u>Cladding</u>	<u>Spacer Disc</u>
UNC-125	4	1	1
UNC-126	3	1	1
UNC-127	3	1	1
UNC-128	3	1	1

A sample of fuel from each of UNC-125 through -128 pins was shipped to INC for burnup determination. Samples of fuel were also taken from these same four pins for testing the equipment installed in the cells for remotely determining O and C.

Twelve cladding specimens, one each from the gas plenum section and the high burnup fuel section, were packaged for shipment to ORNL where additional tests will be carried out as requested by UNC personnel.

Nine capsules (UNC-92, -96, -99, -104, -107, -108, -109, -111, and -112) were received from the EBR-II on September 30. Diagnostic tests will be started on these capsules in October.

VI. REFERENCES

1. E. D. West and K. L. Churney, J. Appl. Phys., 39, 4206 (1968).

PROJECT 463

CERAMIC PLUTONIUM FUEL MATERIALS

Person in Charge: R. D. Baker

Principal Investigator: J. A. Leary  
J. L. Green

I. INTRODUCTION

The principal goals of this project are two-fold. The first is the preparation of pure, well-characterized plutonium containing LMFBR candidate fuel materials and the examination of the irradiation behavior of these materials. The second is the determination of the high temperature properties before and after irradiation of advanced fuel materials prepared by LASL and also of samples of material made available to LASL by DRDT which were prepared and irradiated by other AEC contractors.

The investigations using materials produced at LASL are currently directed toward plutonium containing carbides having compositions that are of interest as advanced fuel forms for the LMFBR program. The irradiation behavior of these materials is being examined under steady state conditions, primarily in the EBR-II reactor. These experiments are designed to investigate fuel swelling, interactions between the fuel and clad and thermal bonding medium, fission gas release, and the migration of fuel material and fission products as a function of burn-up and irradiation conditions.

Properties of interest are: (1) phase relationships using differential thermal analysis, (2) thermal transport, (3) thermal stability and compatibility, (4) hot

hardness and its temperature dependence, (5) structure and phase relationships using high temperature x-ray and neutron diffraction, (6) thermal expansion, and (7) compressive creep rates as a function of temperature and stress.

II. SYNTHESIS AND FABRICATION

(R. Honnell, C. Baker, W. Hayes, G. Moore, and R. Walker)

A program is in progress to develop process procedures for the preparation and fabrication of hyperstoichiometric solid solution (U, Pu)C fuel material. This material is to have approximately 5% sesquicarbide present as a second phase but should contain none of the commonly observed acicular phase.

Avoiding or eliminating the acicular phase in material of this composition is complicated by the fact that the composition of that phase is unknown and the quantities and grain section sizes are too small to allow microprobe or x-ray analysis. An attempt has been made to prepare pellets having the desired composition and microstructure by sintering a blend of single phase  $(U_{0.8}Pu_{0.2})C_{1-x}$  and  $(U_{0.8}Pu_{0.2})C_{1.5}$  powders that are both initially free of acicular phases. Powders having a particle size of  $\leq 0.61 \mu$  were prepared from sintered pellets of known composition and microstructure. Weighed charges of these powders were mixed in a

V-blender and pressed at  $2.1 \times 10^3$  kg/cm<sup>2</sup> into pellets having diameters of 0.736 cm. After sintering, analyzed carbon contents varied from 4.75 to 4.84 wt. %

(U<sub>0.8</sub>Pu<sub>0.2</sub>C<sub>1.0</sub> corresponds to a carbon content of 4.8 wt. %), and oxygen and nitrogen concentrations totaled 600 ppm or less. Four different sintering schedules were employed, i. e., 1900°C for 8h, 1600°C for 24h, 1455°C for 27h, and 1350°C for 22h. Metallographic examination of the sintered pellets indicated the presence of the acicular phase in all cases.

The use of a blended powder technique such as this does not appear to be suitable for the preparation of hyperstoichiometric solid solution monocarbide compositions which are free of the acicular phase.

The fabrication and characterization of single phase (U<sub>0.8</sub>Pu<sub>0.2</sub>)C pellets for use in the EBR-II irradiation assemblies is a continuing effort. In addition, carbide specimens of various compositions are being prepared as required for the property measurement studies.

2. U.S. - U.K. Libby-Cockcroft Oxide Exchange  
(W. M. Jones)

Sintered pellets of (U<sub>0.8</sub>Pu<sub>0.2</sub>)O<sub>2±x</sub> received from the U. K. as part of the Libby-Cockcroft oxide exchange program have been examined metallographically and are currently being chemically analyzed.

III. IRRADIATION TESTING

1. EBR-II Irradiation Testing

The purpose of the EBR-II irradiations is to evaluate candidate fuel/sodium/clad systems for the LMFBR program. In the reference design, fuel pellets of single-phase (U, Pu)C are separated by a sodium bond from a cladding of Type 316 stainless steel. Three series of experiments are planned and approval-in-principle has been received from the AEC. The capsules are to be irradiated under the conditions shown in Table 463 - I.

Results. Two capsules from Series 1, designated K-42B and K-36B have been returned to the LASL hot cells for examination. The capsules accumulated 4.5 at. % and 3.0 at. % burnup for K-42B and K-36B respectively.

Three capsules from Series 1, designated K-37B,

Table 463 - I  
EBR-II Irradiation Conditions

Condition	Series 1	Series 2	Series 3
1. Lineal Power, kW/ft	~ 30	~ 45	~ 30
2. Fuel Composition	(U <sub>0.8</sub> Pu <sub>0.2</sub> )C, single-phase, sintered)		
3. Fuel Uranium	<sup>235</sup> U	<sup>235</sup> U	<sup>235</sup> U
4. Fuel density	90%	85%	95%
5. Smear density	80%	80%	80%
6. Clad size	0.300-in. i.d. x 0.010-in. wall		
7. Clad type	316 SS	316 SS	316 SS
8. Max clad temp, °F	1250	1275	1250
9. Max fuel centerline temp, °F	2130	2550	2100
10. Burnup	3 a/o to 8 a/o		

K-38B, and K-39B, and two capsules from Series 3, designated K-43 and K-44 are currently being irradiated in the EBR-II X086 subassembly at approximately 30 kW/ft. The target burnup for these capsules is 6 to 8 at. %.

The three capsules from Series 2, designated K-49, K-50, and K-51, and two additional capsules from Series 3, designated K-45 and K-46 are available at EBR-II for irradiation. It is expected that these capsules will commence irradiation during the second quarter of FY 1971 in a reconstituted subassembly with some oxide fuels from other experiments.

Two thermal control capsules are operating in an out-of-pile loop. Capsule external temperatures are approximately those of EBR-II in-pile assemblies. One capsule will be removed during the next quarter after an exposure of 6000 hours.

2. Thermal Irradiations of Sodium-Bonded Mixed Carbides  
(J. C. Clifford)

Sodium-bonded mixed carbides are being irradiated in the LASL Omega West Reactor, a 6 MW MTR-type facility, to determine whether fuel, clad, and sodium remain mutually compatible as burnups of interest to the LMFBR program are approached. While fast-spectrum irradiations would be preferable to produce typical power densities and radial temperature gradients anticipated in LMFBRs, thermal irradiations are useful in this instance because the fuel regions of prime interest (those in contact with sodium) for compatibility studies can be maintained at expected LMFBR temperatures.

Fuel for the experiments is  $(U_{0.8}Pu_{0.2})C$ , fully enriched in  $^{235}U$  and containing approximately 4.7 w/o carbon, 270 ppm oxygen, and 370 ppm nitrogen. <sup>(1)</sup>

The material is essentially single phase monocarbide with no higher carbides and approaches 95 per cent of theoretical density. Fuel pellets, 0.265 in. diameter and 0.250 in. thick, are contained in Type 316 stainless steel capsules, each 2.5 in. long and 0.300 in. diameter with a 0.010 in. wall. Each capsule contains three fuel pellets, a stainless steel insulator pellet, and approximately 0.3 grams of sodium. Two such capsules are used in each experiment.

Experiments are conducted in instrumented "environmental cells" installed semi-permanently in the reactor. <sup>(2)</sup> The principal features of these cells are: (1) a heat removal and temperature control system consisting of a natural convection sodium loop, electrical heaters, and a variable conductivity heat leak, and (2) a sweep gas system for the rapid detection of leaking fuel capsules. Fuel surface temperatures are maintained between 600-700°C and predicted centerline temperatures are approximately 180°C higher. Flux depression in the fuel is appreciable, giving rise to fuel power densities which vary from 670 w/g at the surface to 50 w/g at the centerline.

Experiments have been terminated at approximately 4 and 8 at. % surface burnup; barring premature failure, an additional experiment will reach 12 at. % surface burnup in December, 1970. cursory post-irradiation examination of the specimens with 4 and 8 at. % burnup has not revealed any significant deleterious effects on compatibility. As might be anticipated in view of the low fuel centerline temperatures, there was no detectable gross fission product migration within the fuel. Aside from cracking, particularly at the longer exposure, the fuel did not undergo any significant observable changes. Additional phases were not seen in the high burnup regions and, although sodium logging was apparent throughout the fuel pellets, no evidence of attack by sodium was detected. Capsule material from the experiments was distinguished from out-of-pile controls primarily by a wide variation in etching response

of material along the inner surfaces of the irradiated capsules. Judging from optical metallographic and autoradiographic examinations of the capsules there has been some limited, non-uniform transfer of fuel constituents to the cladding. Plutonium was present along the capsule inner surfaces, and carbon penetrated as much as a tenth of the wall thickness at isolated locations. Electron beam microprobe examinations in progress may amplify these observations.

#### IV. PROPERTIES

##### 1. Differential Thermal Analysis

(J. G. Reavis, L. Reese)

A sample of irradiated  $UO_2 - 20\% PuO_2$  was sealed in a W capsule and examined using DTA over the range 1300 to ~2900°C. Additional determinations have been made of transformation temperatures in the Pu-C system by application of DTA and quenching techniques. Transformations of  $(U, Pu)C$  and  $(U, Pu)C_2$  have also been investigated.

##### DTA of Irradiated Samples:

Previous DTA observations of irradiated fuel materials were carried out in open crucibles. These experiments were complicated by difficulties caused by volatile fission products. The use of those results in describing the properties of an encapsulated irradiated fuel in-reactor is questionable since the volatilization of fission products resulted in composition changes during the measurements.

Recent DTA measurements have been made on specimens sealed in W capsules having reentrant wells for optical pyrometric temperature measurement. Melting of  $ZrO_2$  in a sealed capsule showed that the temperature correction curve currently used is valid to  $\pm 20^\circ$  at 2685°C.

A sample of irradiated  $UO_2 - 20\% PuO_2$  sealed in a W capsule has been cycled several times through melting. The sample was taken from the central region of a fuel pin which had been irradiated in EBR-II to 57,000 MWD/MTM (NUMEC B-9-56). No thermal arrests were detected below 2685°C. Solidus and liquidus temperatures for this material were observed at  $2725 \pm 30^\circ$  and  $2825 \pm 30^\circ$  C. These are compared in Table 463 - II with reference values for unirradiated

UO<sub>2</sub> - 20% PuO<sub>2</sub>.

Table 463 - II

Solidus and Liquidus Temperatures of UO <sub>2</sub> - 20% PuO <sub>2</sub> Observable in Sealed Tungsten Capsules		
Reference	Solidus °C	Liquidus °C
This work	2725 ± 30	2825 ± 30
Ref. 3	2787 ± 25	2855 ± 25
Ref. 4 - (observed)	2760 ± 20	2790 ± 20
Ref. 4 (graph)	2740	2775
Ref. 5	2780 ± 20	2820 ± 20

Comparison of values listed in Table 463 - II shows that the solidus and liquidus temperatures of the irradiated material are somewhat lower than those of comparable unirradiated specimens, but the differences are within the uncertainty of the determination.

Although the prominent, reproducible thermal arrest exhibited by the irradiated material was at 2725°C, a weak, non-reproducible irregularity was observed on less than half of the heating cycles at 2685°C. The fact that this irregularity was seen dictates that replicate measurements be made on the irradiated material. In addition, comparison samples of archival materials will be examined.

Pu-C Transformations:

The results of transformation temperature determinations for Pu-C compositions are listed in Table 463 - III. These values are in generally good agreement with previous observations. The horizontal phase boundaries and liquidus temperatures for compositions having C/Pu atomic ratios greater than 1.0 now appear to be well-defined. The vertical "dicarbide" phase boundary is very close to PuC<sub>2.00</sub> and the high C limit of sesquicarbide is very close to 1.50. The low C limit of sesquicarbide appears to be a function of temperature and is less well-defined. The best composition of "single phase" monocarbide above 1000°C appears to be PuC<sub>0.87</sub>, but the vertical phase boundaries are not well known. The remaining unknown phase boundary of the Pu-C system appears to be the liquidus line between PuC<sub>0.1</sub> and PuC<sub>0.3</sub>.

U-Pu-C Transformations:

A brief search was made for a transformation of U<sub>0.65</sub>Pu<sub>0.35</sub>C<sub>2</sub> (excess C) near 1550°C by metallographic examination of microstructures of samples quenched from 1800, 1650, and 1450°C. The specimen had been previously annealed at 2200°C and slow-cooled to 1800°C at the beginning of the series. Quenching rates were of the order of 1000 deg/min. The 1800°C specimen showed a typical "dicarbide" structure as would be expected for this composition quenched from above the 1740°C transformation. The specimens quenched from 1650 and 1450°C both contained sesquicarbide and graphite, and were not significantly different from each other. These observations do not lend support to the indication of a transformation at 1550°C as shown by high temperature x-ray diffraction measurements. (6)

Table 463 - III

Transformations Observed in Pu-C Compositions

C/Pu Atom Ratio	Thermal Arrests °C	Liquidus, °C
0.72	----	1680
0.76	----	1695
0.82	1580	1695
0.94	1585	>1760
0.96	1590	>1785
1.52	1655, 1995	<2045
1.91	1655, 2015	<2230

Solidus and liquidus temperatures of two additional mixed uranium-plutonium monocarbide compositions have been determined from DTA measurements. Solidus and liquidus values found for U<sub>0.4</sub>Pu<sub>0.6</sub>C were 1905 and 2260°C respectively. Solidus and liquidus values for U<sub>0.3</sub>Pu<sub>0.7</sub>C were 1825 and 2200°C respectively. These liquidus values are higher than expected from extrapolation of previous results, indicating even higher heats of fusion of UC and PuC than the 20 and 10 kcal/mole, respectively, which were estimated using ideal solution theory to fit the experimental data. The transition temperatures reported above, therefore, imply even higher values for entropies of fusion than were calculated from the data reported earlier. Even the earlier entropies of fusion were substantially larger than would normally be regarded as nominal for mono-



carbides. This seems to indicate that the melting of the mixed uranium-plutonium monocarbides is a more complicated process than is accounted for by the ideal solid and liquid solution model being considered.

## 2. Room Temperature X-ray Diffraction (C. W. Bjorklund)

The results of the characterization of plutonium fuel materials by room temperature x-ray powder diffraction techniques have been incorporated in other sections of this report.

Periodic measurements of the lattice expansion induced by self-irradiation damage in samples of PuO<sub>2</sub> containing 3.75 at. % <sup>238</sup>Pu at elevated temperatures (100, 200, and 400°C) have been discontinued. The lattice dimensions have been constant for several years, and no evidence of significant line broadening has been detected. The samples will be retained in their original capillaries at room temperature to determine whether additional expansion to the room temperature saturation values will occur. The lattice dimensions of PuO<sub>2</sub>, PuN and Pu<sub>2</sub>C<sub>3</sub> of normal isotopic composition measured almost a year after the previous set of measurements all showed a continued slow increase despite the fact that the samples are now between 5 and 7 years old.

A precision linear comparator currently in use for some of the powder diffraction film measurements is constructed in such a manner that it would be possible to add a photoelectric scanning device with an automatic readout of the line positions and densities. This potential was evaluated through the cooperation of the emission spectroscopy research section of the analytical chemistry group. A slit densitometer device was used to scan an x-ray film of a two-phase Pu carbide of less than average quality (for which problems are encountered when visual measurements are made). The high angle end of the film was used, since the device could scan only a length of the x-ray film which was slightly less than half the overall length of the film. Thus, shrinkage corrections and lattice dimensions could not be calculated, but the ring diameters of poorly resolved reflections could be detected and measured. The results were quite encouraging for precision measurements. Conceivably standardization of such options as

slit widths and measuring intervals could be made to minimize the time required and perhaps make the technique applicable to routine measurements. The alternate rotating prism technique with line profiles displayed on the screen of an oscilloscope is also available, but has not been tested. The latter technique might be considerably faster for routine measurements.

## 3. Boron Carbide Structural Study (K. L. Walters, J. L. Green)

The preliminary neutron diffraction data <sup>(6)</sup> indicated that the boron carbide structure differed from that suggested by Clark and Hoard <sup>(7)</sup> only in the location of the various atoms. For the material examined, a composition of B<sub>13</sub>C<sub>2</sub> or possibly B<sub>5</sub>C appeared most consistent with the crystallographic results.

The stoichiometry B<sub>13</sub>C<sub>2</sub> has been postulated by other workers for boron carbide, but considerable uncertainty exists in this area. The question regarding the stoichiometry of the unit cell as determined from the neutron diffraction data results from the uncertainty associated with the average scattering length calculated for the boron atoms in the icosahedral groups. This problem should be greatly reduced by the acquisition of more data, a process now largely completed. It then may be possible to determine average scattering lengths with sufficient confidence to determine whether or not a vacancy exists in the boron icosahedra in the structure.

A major difficulty in boron carbide work to date has been the lack of a satisfactory analytical method for the determination of free graphite. Of the analytical techniques reported in the literature <sup>(10-14)</sup> the recent work of Gokhshteen <sup>(13)</sup> is of particular importance. A variation of that procedure is currently being evaluated at LASL. An independent chemical determination of the composition of the boron carbide phase would be extremely valuable.

As a check on the original LASL boron carbide x-ray data, <sup>(6)</sup> comparisons have been made with diffraction data recently reported by ORNL. <sup>(15)</sup> A twenty line boron carbide pattern essentially identical to the LASL line test was extracted from that data. It would appear that at least one impurity phase in addition to graphite was also present in the samples used in the

ORNL study.

Additional areas in which investigations are being initiated include (1) single crystal x-ray studies for refinement of position parameters, for atom identity determinations, and also to test the possibility of long range defect ordering, (2) examination by neutron diffraction of a boron-rich boron carbide sample, and (3) examination by neutron diffraction of irradiated boron carbide.

Difficulty has been experienced in attempting to purchase boron carbide of purity similar to that used to date. It appears that the material used in the x-ray and neutron studies was of exceptional purity. The general lack of high purity boron carbide has probably been the primary cause for the difficulties in crystallographic analysis that have been reported in the literature.

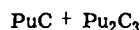
#### 4. Mass Spectrometric Studies of the Vaporization of Pu Compounds (R. A. Kent)

Among the parameters required for the design of fuel materials for fast breeder reactors are the thermodynamic properties of these materials at high temperatures. From these properties, the stabilities of these materials with respect to the cladding may be calculated in addition to the activities of the individual components. Included among the fuel forms being considered are the mixed uranium-plutonium carbides. This study of the vaporization behavior of the binary Pu-C system was undertaken as an initial step in the investigation of the U-Pu-C ternary system.

Our study of the vaporization behavior of the Pu-C system has been completed and some of the preliminary results have been published.<sup>(16, 17, 18)</sup> In this report the results obtained in this study are compared with those obtained in various other investigations.<sup>(17-22)</sup>

##### a.1 Vapor pressure results:

The results of this investigation indicate that there are four composition regions of the Pu-C phase diagram which give rise to invariant but non-congruent vaporization: monocarbide plus sesquicarbide, sesquicarbide plus carbon, sesquicarbide plus dicarbide, and dicarbide plus carbon. The vapor species produced above each of these regions is gaseous Pu and the results are discussed below.

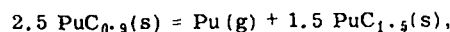


The vapor pressure of Pu(g) above this two-phase region is given by

$$\log_{10} P_{\text{Pu}} \text{ (atm)} = (5.118 \pm 0.027) - (18,919 \pm 72)/T^{\circ}\text{K},$$

$$(1450-1848^{\circ}\text{K}) \quad (1)$$

For the decomposition reaction



the free energy is given by

$$\Delta G_T = 86,570 - 23.42 T, \text{ (cal/mole)}. \quad (2)$$

The vapor pressure results obtained for this region of the phase diagram by the various investigators are compared in Table 463 - IV.

Table 463 - IV

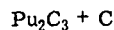
Vapor Pressure Data for the Reaction  
2.5 PuC<sub>0.9</sub>(s) = Pu(g) + 1.5 PuC<sub>1.5</sub>(s)

Temp., °K	Pressure P <sub>Pu</sub> (atm) This Work	Relative Pu Pressures (This Work/Other Data)		
		Ref. 19	Ref. 20	Ref. 22
1500	3.20 x 10 <sup>-4</sup>	0.95	0.76	5.48
1600	1.97 x 10 <sup>-7</sup>	0.93	0.82	5.55
1700	9.75 x 10 <sup>-7</sup>	0.91	0.88	5.60
1800	4.05 x 10 <sup>-6</sup>	0.90	0.94	5.66
1900	1.45 x 10 <sup>-4</sup>	0.88	0.99	5.71

$\Delta G_{1873^{\circ}\text{K}}$  for the Decomposition Reaction

42.7	kcal/mole	this work
42.2	kcal/mole	ref. 19
42.6	kcal/mole	ref. 20
49.2	kcal/mole	ref. 22

The results listed in Table 463 - IV indicate good agreement in the range 1700-1900°K between three sets of data, obtained employing different techniques. The data of Marcon<sup>(22)</sup> are lower by a factor of about six and may be considered to be in error inasmuch as the data from this study yield results in good agreement with low temperature calorimetric studies as noted below.

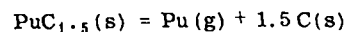


The pressure of Pu(g) above this two-phase region is given by

$$\log_{10} P_{\text{Pu}} \text{ (atm)} = (4.468 \pm 0.057) - (20,598 \pm 106)/T^{\circ}\text{K},$$

$$(1668-1927^{\circ}\text{K}). \quad (3)$$

For the decomposition reaction



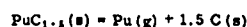
the free energy is given by

$$\Delta G_T = 94,252 - 20.44 T, \text{ (cal/mole)}. \quad (4)$$

The results obtained from this investigation are compared with those from other studies in Table 463 - V.

Table 463 - V

Vapor Pressure Data for the Reaction

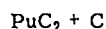


Temp., °K	Pressure Pu (atm)	Relative Pu Pressures (This Work/Other Data)		
	This Work	Ref. 19	Ref. 21	Ref. 22
1600	$3.93 \times 10^{-8}$	1.23	0.38	0.98
1700	$2.25 \times 10^{-8}$	1.20	0.41	1.01
1800	$1.06 \times 10^{-7}$	1.18	0.46	1.04
1900	$4.24 \times 10^{-7}$	1.16	0.46	1.07

$\Delta G_{1973^\circ\text{K}}$  for the Decomposition Reaction

54.7	kcal/mole	this work
54.2	kcal/mole	ref. 19
57.7	kcal/mole	ref. 21
55.0	kcal/mole	ref. 22

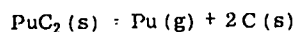
The data listed in Table 463 - V show satisfactory agreement between the results of this study and those from two others. The usual experimental uncertainty in measurements of this type is less than  $\pm 20\%$ . The vapor pressure of Battles et. al. <sup>(21)</sup> are lower by a factor of about two, which leads to a difference in  $\Delta G$  of about 3 kcal/mole. This difference cannot be resolved until the high temperature calorimetry data are available. It should be noted, however, that most of the experimental errors encountered in vapor pressure measurements lead to too low pressure values.



The Pu (g) pressure above this two-phase region is given by the equation

$$\log_{10} P_{\text{Pu}} (\text{atm}) = (3.787 \pm 0.084) - (19,288 \pm 170)/T^\circ\text{K}, \quad (1933-2140^\circ\text{K}). \quad (5)$$

The free energy for the decomposition reaction



is given by

$$\Delta G_T = 88,258 - 17.33 T, (\text{cal/mole}). \quad (6)$$

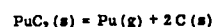
The various vapor pressure data for this reaction are listed in Table 463 - VI and are not in as good agreement as those for the other decomposition reactions.

Some of the discrepancies may be resolved once the high temperature heat content data are available. The various values for the free energy of the decomposition at  $1933^\circ\text{K}$  agree with each other within  $\pm 3$

kcal/mole. Again the vapor pressure data of Battles, et. al. <sup>(21)</sup> are lower by a factor of about two.

Table 463 - VI

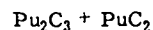
Vapor Pressure Data for the Reaction



Temp., °K	Pressure Pu (atm)	Relative Pu Pressures (This Work/Other Data)		
	This Work	Ref. 20	Ref. 21	Ref. 22
2000	$1.39 \times 10^{-6}$	1.29	0.46	1.17
2100	$4.00 \times 10^{-6}$	1.25	0.46	1.25
2200	$1.05 \times 10^{-5}$	1.21	0.46	1.32
2300	$2.52 \times 10^{-5}$	1.18	0.46	1.39

$\Delta G_{1933^\circ\text{K}}$  for the Decomposition Reaction

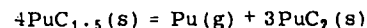
54.8	kcal/mole	this work
53.7	kcal/mole	ref. 20
57.8	kcal/mole	ref. 21
55.2	kcal/mole	ref. 22



The pressure of Pu (g) above this two-phase region is given by

$$\log_{10} P_{\text{Pu}} (\text{atm}) = (6.533 \pm 0.109) - (24,569 \pm 223)/T^\circ\text{K}, \quad (1933-2170^\circ\text{K}). \quad (7)$$

For the decomposition reaction



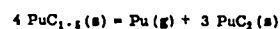
the free energy is given by

$$\Delta G_T = 112,423 - 29.89 T, (\text{cal/mole}). \quad (8)$$

The data from this work are compared to those from other studies in Table 463 - VII. There is good agreement between the results of this study and those of Marcon. <sup>(22)</sup> Again, the vapor pressure data of Battles, et. al. <sup>(21)</sup> are lower by a factor of two, although the value of  $\Delta G$  at  $1933^\circ\text{K}$  for the decomposition reaction is in fair agreement.

Table 463 - VII

Vapor Pressure Data for the Reaction



Temp., °K	Pressure Pu (atm)	Relative Pu Pressures (This Work/Other Data)	
	This Work	Ref. 21	Ref. 22
2000	$1.77 \times 10^{-6}$	0.49	1.12
2100	$6.82 \times 10^{-6}$	0.53	1.08
2200	$2.31 \times 10^{-5}$	0.57	1.05
2300	$7.09 \times 10^{-5}$	0.60	1.02

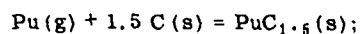
$\Delta G_{1933^\circ\text{K}}$  for the Decomposition Reaction

54.6	kcal/mole	this work
57.6	kcal/mole	ref. 21
55.1	kcal/mole	ref. 22

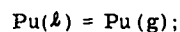
## a.2 Free Energies of Formation



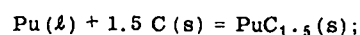
If the free energy expression for the decomposition of the sesquicarbide, eq (4), is combined with that for the vaporization of Pu metal<sup>(23)</sup> at 1842°K, the average temperature for the sesquicarbide decomposition data, we have



$$\Delta G = -94,252 + 20.44 T, \text{ (cal/mole)}$$



$$\Delta G = 80,157 - 22.63 T, \text{ (cal/mole)}$$



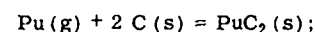
$$\Delta G_{f1842} = 14,095 - 2.19 T, \text{ (cal/mole)}. \quad (9)$$

Equation (9) cannot be corrected to 298°K until high temperature heat content data become available. A sample of single phase  $\text{PuC}_{1.5}$  has been supplied to ANL for a determination of  $\Delta H_{f298}$  by means of oxygen bomb calorimetry.

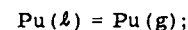
Equation (9) when extrapolated to 1000°K, yields  $\Delta G_f = -16.3$  kcal/mole, the same value as that obtained from the emf study performed in this laboratory.<sup>(17, 18)</sup>



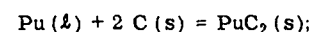
If the free energy expression for the decomposition of the dicarbide, eq (6), at the average temperature of the data, 2026°K, is combined with that for the vaporization of Pu metal at the same temperature,<sup>(23)</sup> we have



$$\Delta G = -88,258 + 17.33 T, \text{ (cal/mole)}$$



$$\Delta G = 80,687 - 22.90 T, \text{ (cal/mole)}$$

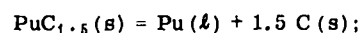


$$\Delta G_{f2026} = -7,571 - 5.57 T, \text{ (cal/mole)}. \quad (10)$$

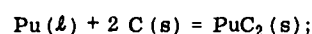
Again, eq (10) cannot be corrected to 298°K until the high temperature heat content data are available.

### Transformation Temperature

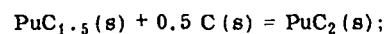
If the free energy expressions for the formation of the sesquicarbide and the dicarbide hold at the transition temperature, we have, combining equations (9) and (10),



$$\Delta G = 14,095 + 2.19 T, \text{ (cal/mole)}$$



$$\Delta G = -7,571 - 5.57 T, \text{ (cal/mole)}$$



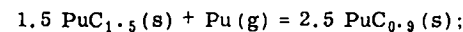
$$\Delta G_{\text{trans}} = 6,524 - 3.38 T, \text{ (cal/mole)}. \quad (11)$$

Equation (11) yields a transition temperature of 1930°K (1657°C) in excellent agreement with the value,  $1660 \pm 10^\circ\text{C}$ , obtained from DTA studies performed in this laboratory.<sup>(24)</sup>

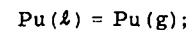
If the free energy expressions obtained in this study are internally consistent, the values of  $\Delta G$  given by equations (4), (6), and (8) should all be equal at the sesquicarbide to dicarbide transition temperature, 1933°K. This criterion is satisfactorily met as the values calculated at 1933°K from these equations are  $54.7 \pm 0.6$ ,  $54.8 \pm 0.9$ , and  $54.6 \pm 1.1$  kcal/mole respectively.



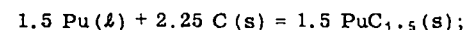
If the expressions for the decomposition of the monocarbide, eq (2), and the formation of the sesquicarbide, eq (9), are combined with that for the vaporization of Pu metal at 1662°K,<sup>(23)</sup> we can obtain the expression for the free energy of formation of the monocarbide. As noted above, we do not have the necessary heat content data to enable us to calculate  $\Delta G_f$  for the sesquicarbide at 1662°K. However, we do have  $\Delta G_f$  values at 1842°K from this work and at 1000°K from the emf study.<sup>(17, 18)</sup> Interpolating, we have at 1662°K



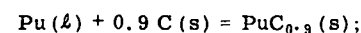
$$\Delta G = -86,570 + 23.42 T, \text{ (cal/mole)}$$



$$\Delta G = 79,716 - 22.38 T, \text{ (cal/mole)}$$



$$\Delta G = -21,952 - 2.84 T, \text{ (cal/mole)}$$



$$\Delta G_{f1662} = -11,522 - 0.72 T, \text{ (cal/mole)}. \quad (12)$$

Equation (12) extrapolated to 1000°K yields  $\Delta G_f = -12.2$  kcal/mole, as compared to the value,  $-12.5$  kcal/mole, obtained from the emf data.<sup>(17, 18)</sup>

When eq (12) is reduced to 298°K by combination with published thermodynamic functions for Pu(l),<sup>(13, 25)</sup> C(s)<sup>(26)</sup> and PuC<sub>0.9</sub>,<sup>(27)</sup> we obtain for PuC<sub>0.9</sub>(s),  $\Delta H_{f298}^{\circ} = -10.9$  kcal/mole,  $\Delta S_{f298}^{\circ} = +2.9$  eu, and  $S_{298}^{\circ} = 17.3$  eu. These results are in excellent agreement with those obtained from calorimetric studies,  $\Delta H_{f298}^{\circ} = -11.4$  kcal/mole<sup>(28)</sup> and  $S_{298}^{\circ} = 17.33$  eu.<sup>(27)</sup>

### a.3 Activities

Aside from the free energy expressions, the parameters of most importance in predicting reactions between the fuel material and the clad and/or fission products, are the activities of the individual components of the fuel. The vapor pressure data obtained in this investigation and the data from the emf study<sup>(17, 18)</sup> were combined to yield Pu activities as a function of composition. The carbon activities were then calculated by means of a Gibbs-Duhem integration.

Activities of Pu and C as a function of composition at 1800°K are listed in Table 463 - VIII. When the temperature is reduced to 1000°K, the values for the composition PuC<sub>1.0</sub> are  $A_{Pu} = 0.05$  and  $A_C = 0.06$ . The values at 1000°K for the composition PuC<sub>1.5</sub> are  $A_{Pu} = 0.0002$  and  $A_C = 1.0$ .

Table 463 - VIII

Activity Values for Pu and C at 1800°K		
Condensate	$A_{Pu}$	$A_C$
PuC <sub>0.70</sub>	0.95	0.02
PuC <sub>0.76</sub>	0.85	0.03
PuC <sub>1.00</sub> (PuC + Pu <sub>2</sub> C <sub>3</sub> )	0.23	0.11
PuC <sub>1.45</sub>	0.11	0.15
PuC <sub>1.50</sub> (Pu <sub>2</sub> C <sub>3</sub> + C)	0.006	1.00

### b.1 Uranium - Plutonium - System

As it was noted above, the primary purpose for the investigation of the Pu-C binary system was to lay the groundwork for an investigation of the U-Pu-C ternary system. Of special interest are compositions near the stoichiometry U<sub>0.8</sub>Pu<sub>0.2</sub>C<sub>1.0</sub>. One area of concern with respect to the U-Pu-C system is that if two condensed phases are present, one of these phases may become significantly richer in Pu. Although few experimental

data are available for the U-Pu-C ternary system, enough data do now exist for the U-C and Pu-C binary systems to allow us to make some calculations and semi-quantitative predictions about the U-Pu-C system. For the following calculations, the free energy expressions for the Pu-C compositions are from this work, those for U and U-C compositions are from Storms<sup>(29)</sup> and those for Pu are from Rand.<sup>(25)</sup>

### b.2 Monocarbide Plus Liquid

Consider a composition U<sub>x</sub>Pu<sub>1-x</sub>C<sub>y</sub>, where  $1 > y > 0$ , consisting of two phases,

$$U_{x_1}Pu_{1-x_1}C_{1.0}(s) \text{ and } U_{x_2}Pu_{1-x_2}(l).$$

For U<sub>x<sub>1</sub></sub>Pu<sub>1-x<sub>1</sub></sub>C<sub>1.0</sub>(s) we have

$$\Delta G_1 = x_1 \Delta G^{\circ} UC(s) + (1-x_1) \Delta G^{\circ} PuC(s) + RT [x_1 \ln x_1 + (1-x_1) \ln (1-x_1)].$$

For U<sub>x<sub>2</sub></sub>Pu<sub>1-x<sub>2</sub></sub>(l) we have

$$\Delta G_2 = x_2 \Delta G^{\circ} U(l) + (1-x_2) \Delta G^{\circ} Pu(l) + RT [x_2 \ln x_2 + (1-x_2) \ln (1-x_2)].$$

If these two phases are in equilibrium, the free energy of the system will be a minimum and

$$\frac{\partial}{\partial x_1} (\Delta G_1)_T = \frac{\partial}{\partial x_2} (\Delta G_2)_T.$$

Thus we have

$$RT \ln (1-x_1/x_1)(x_2/1-x_2) = \Delta G^{\circ} UC(s) - \Delta G^{\circ} PuC(s) - \Delta G^{\circ} U(l) + \Delta G^{\circ} Pu(l). \quad (13)$$

Equation (13) was employed to calculate the values listed in Table 463 - IX, where x<sub>1</sub> refers to the mole fraction of U in the monocarbide and x<sub>2</sub> to the mole fraction of U in the liquid. The results listed in Table 463 - IX are only approximate ones, as at high temperatures the solubility of C in the liquid will increase and this should be taken into account. However, the results do indicate that the liquid will be significantly richer in Pu. This phenomenon is more pronounced at the lower temperatures and at higher Pu contents, as might be expected from a comparison of the melting points, 913°K for Pu, and 1406°K for U.

If we have an initial monocarbide composition U<sub>0.8</sub>Pu<sub>0.2</sub>C<sub>y</sub> in equilibrium with liquid at 1800°K, the liquid composition will be about U<sub>0.17</sub>Pu<sub>0.83</sub> and the vapor pressures would be approximately 1.4 x 10<sup>-5</sup> atm for Pu and 2 x 10<sup>-10</sup> atm for U. The corresponding

corresponding activities would be,  $A_{Pu} = 0.8$ ,  $A_U = 0.05$ , and  $A_C = 0.01$ .

### b.3 Monocarbide Plus Sesquicarbide

Consider a composition  $U_xPu_{1-x}C_y$ , where  $1.5 > y > 1.0$ , consisting of two phases,  $U_{x_1}Pu_{1-x_1}C_{1.0}(s)$  and  $U_{x_2}Pu_{1-x_2}C_{1.5}(s)$ . If we make a calculation similar to that for the case, monocarbide plus liquid, we have, if the monocarbide and sesquicarbide coexist in equilibrium,

$$RT \ln (1-x_1/x_1)(x_2/1-x_2) = \Delta G^{\circ} UC(s) - \Delta G^{\circ} PuC(s) - \Delta G^{\circ} UC_{1.5}(s) + \Delta G^{\circ} PuC_{1.5}(s). \quad (14)$$

Equation (14) was employed to calculate the values listed in Table 463 - X where  $x_1$  refers to the mole fraction of U in the monocarbide and  $x_2$  to that in the sesquicarbide. The data in Table 463 - X indicate that, again, the monocarbide becomes poorer in Pu.

At 1800°K the Pu pressure above the overall composition  $U_{0.8}Pu_{0.2}C_y$ , consisting of monocarbide and sesquicarbide, will be about  $8 \times 10^{-7}$  atm. The activities would be approximately  $A_{Pu} = 0.04$ ,  $A_U = 0.005$ , and  $A_C = 0.02$ .

Note that by moving in composition from the two-phase mixture, MC + liquid, to the two-phase mixture MC +  $M_2C_3$ , we obtain a much lower Pu activity without an appreciable increase in the carbon activity. As long as the sample consists mostly of monocarbide with a small amount of sesquicarbide, and as long as the temperature is low enough to prevent formation of the dicarbide, the C activity will remain low.

The mole fractions calculated and listed in Tables 463 - IX and - X, as well as the activities calculated from these values, are only approximate. More

Table 463 - IX

#### Monocarbide Plus Liquid

Temp. °K	Values of $x_2$ for Given Values of $x_1$ *								
	$x_1 = 0.1$	0.2	0.3	0.4	0.5	0.6	0.7	0.8	0.9
1600	0.003	0.008	0.01	0.02	0.03	0.04	0.07	0.11	0.22
1800	0.006	0.012	0.02	0.03	0.05	0.07	0.10	0.17	0.31
2000	0.008	0.018	0.03	0.05	0.07	0.10	0.15	0.23	0.40

\*  $x_1$  is the mole fraction of U in the monocarbide and  $x_2$  is the mole fraction of U in the liquid.

Table 463 - X

#### Monocarbide Plus Sesquicarbide

Temp. °K	Values of $x_2$ for Given Values of $x_1$ *								
	$x_1 = 0.1$	0.2	0.3	0.4	0.5	0.6	0.7	0.8	0.9
1600	0.05	0.10	0.16	0.23	0.31	0.40	0.51	0.64	0.80
1800	0.05	0.11	0.17	0.24	0.32	0.42	0.52	0.66	0.81
2000	0.05	0.11	0.18	0.25	0.33	0.43	0.54	0.66	0.82

\*  $x_1$  is the mole fraction of U in the monocarbide and  $x_2$  is the mole fraction of U in the sesquicarbide.

accurate determinations of these numbers will become available as we obtain more data for the U-Pu-C system.

### c. Miscellaneous

A number of modifications of the RM6-K magnetic mass spectrometer have been or are being made.

1. The 10-stage multiplier has been replaced with a 16-stage unit, thus increasing the sensitivity by a factor of about 100.

2. Changes in the pumping system, necessary to accommodate the glove box, are being made. The various component pieces are being made in the LASL shops.

3. The ion source is being modified to allow RPD measurements.

4. The Hitachi ion gauges and Geissler discharge tubes have been replaced with standard U. S. ion and thermocouple gauges. If the glove box is delivered on schedule, we anticipate that the RM6-K unit will be in operation with Pu-containing samples by February, 1971.

Once the RM6-K unit is in operation, all thermodynamic studies of the U-Pu-C system will be made with that apparatus. The older quadrupole unit is being modified for the study of post-irradiated samples. These modifications will allow us to study the release of tritium and of fission product gases from irradiated fuel and clad materials at high temperatures.

### 6. High Temperature Calorimetry (D. G. Clifton)

The drop calorimeter located in the LASL hot cells is now operative. A number of electrical calibrations have been made when the system contains argon. Further experiments are necessary on empty tungsten capsule drops before data can be acquired for irradiated fuel samples.

A 45 gm sample of an irradiated  $\text{UO}_2$ -20%  $\text{PuO}_2$  fuel element, NUMEC B-9-56, that has had a fast flux exposure of about 57,000 MWD/Te has been welded into a W capsule. A self-heating measurement was recorded for this sample, but the data has not been reduced.

This capsule has since been opened, 5 gms of material removed for additional DTA measurements, and the remaining 40 gms sealed into another W capsule. Efforts are underway to complete measurements on this material. An archival sample of this material has been

obtained. A portion of this will be encapsulated and used for comparison measurements in the hot cell calorimeter.

Procedural changes in the operation of the drop calorimeter used with unirradiated materials has made it necessary to repeat some of the apparatus calibration measurements. The sight-port window corrections that are used for the optic pyrometer observations have been redetermined. The calorimeter is presently being operated with an argon atmosphere at about -3" of Hg pressure to speed up the heat transfer and consequent equilibration of the system. This has necessitated new heat leak determinations, electrical calibrations and empty tungsten capsule drops. Several of these tasks have been completed.

No heat content measurements for PuN or  $\text{Pu}_2\text{C}_3$  have been reported in the literature to date. Samples of these two materials are available and have been prepared for enthalpy studies. A 55.23 gm sample of PuN.<sub>944</sub> has been put into the calorimeter and a self-heating measurement has been made. The value obtained was  $2.27 \times 10^{-3}$  watts/gm Pu.

High temperature drops of the PuN.<sub>994</sub> sample have been made at 1590 and 1744°K. A preliminary reduction of the data for the 1590°K drop gives a value for  $H_T^0 - H_{293}^0$  of 18.8 kcal/mole. This compares favorably with 18.2 kcal/mole, which is an estimated value given by Kent and Leary.<sup>(30)</sup> The set of data at 1744°K has not yet been reduced.

### 7. Compressive Creep (M. Tokar)

Results obtained on the compressive creep of specimens having the composition  $\text{U}_{0.79}\text{Pu}_{0.21}\text{C}_{1.02}$  are summarized in Table 463 - XI. UC data, taken from Stellrecht, et. al.<sup>(31)</sup> are shown for comparison. It is apparent that the UC had greater creep resistance (lower creep rates) than the mixed carbide. The difference in creep behavior might be due to the low density (~ 87% theoretical) of the sintered  $\text{U}_{0.79}\text{Pu}_{0.21}\text{C}_{1.02}$  specimens; Stellrecht's UC specimens were arc-cast rods.

From the creep rates listed in Table 463 - XI the apparent activation energy for creep of  $\text{U}_{0.79}\text{Pu}_{0.21}\text{C}_{1.02}$  is calculated to be approximately 120 kcal/mole. In a

Table 463 - XI

Creep Rates of UC and  $U_{0.79}Pu_{0.21}C_{1.02}$ 

Temp. (°C)	Pressure (psi)	Creep Rate ( $\dot{\epsilon}$ )	
		$U_{0.79}Pu_{0.21}C_{1.02}$	UC*
1300	2000	$2.43 \times 10^{-5} h^{-1}$	$1 \times 10^{-5} h^{-1}$
--	4000	$1.07 \times 10^{-4} h^{-1}$	$4.5 \times 10^{-5} h^{-1}$
--	6000	$4.05 \times 10^{-4} h^{-1}$	$1.2 \times 10^{-4} h^{-1}$
1400	2000	$3.29 \times 10^{-4} h^{-1}$	$4.1 \times 10^{-5} h^{-1}$
--	4000	$1.39 \times 10^{-3} h^{-1}$	$4 \times 10^{-4} h^{-1}$
1500	2000	$2.84 \times 10^{-3} h^{-1}$	$8 \times 10^{-5} h^{-1}$

\* Taken from Stellrecht et al. (31) Since Stellrecht et al. did not use the same temperature and pressure ranges used in this study, some of the UC creep rates listed here are extrapolated or interpolated values.

recent paper (32) the activation energy for creep of  $U_{0.79}Pu_{0.21}C_{1.02}$  was reported to be  $100 \pm 10$  kcal/mole. The creep rates for  $U_{0.85}Pu_{0.15}C$  were reported to be higher than those for UC (31) or for UN, (33) and this was tentatively attributed to the relatively high porosity (~ 9%) of the  $U_{0.85}Pu_{0.15}C$  specimens used in that study. It should be noted that the effects of microstructural variables on the creep rates of UC or solid solution (U, Pu)C have not as yet been established even semi-quantitatively.

In another recent paper, Killey, et al. (34) reported on the compressive creep of UC and  $U_{0.85}Pu_{0.15}C$ . The mixed carbide was tested in the temperature range  $1080 - 1180^{\circ}C$  and the deformation rates were reported to be comparable to those for UC. The activation energy was reported as being on the order of 100 kcal/mole. There was considerable scatter in the data, however, and this was later attributed to differences in microstructure or composition in the specimens, which were not all prepared at one time. (35) It should be noted that in the present study all the specimens currently being tested were prepared from one batch of material and were sintered at the same time. In this way, unintentional variations in microstructure and composition can be minimized.

Creep data are usually used to determine a general creep equation of the form

$$\dot{\epsilon} = A \sigma^n e^{-Q/RT}$$

where:

$\dot{\epsilon}$  = creep rate (in this case in inches/inches/hour)

A = a constant

$\sigma$  = stress (psi)

n = stress exponent

$e^{-Q/RT}$  = Arrhenius expression

The data obtained to date on  $U_{0.79}Pu_{0.21}C_{1.02}$  yield a stress exponent of 2.1 to 2.6 as compared to  $n \approx 2.3$  reported for  $U_{0.85}Pu_{0.15}C$ .

#### Hot Hardness

A new furnace has been installed in the hot hardness tester. This required modifications of the cooling water and vacuum systems. The unit is now undergoing vacuum leak checks prior to being calibrated.

#### 8. Transport Properties

(K. W. R. Johnson and J. F. Kerrisk)

##### Thermal Diffusivity

The thermal diffusivity laser equipment and high temperature furnace have been moved into position for non-radioactive operation. This setup of the diffusivity equipment will simulate the relative location of the furnace and laser when the furnace is installed in a glove box. It will permit operation with non-plutonium samples to the maximum operating temperature of the furnace. Operation is awaiting service connections to the furnace.

Preliminary room temperature diffusivity measurements were started with samples in place in the furnace. Some laser beam energy nonuniformity was observed in the new setup. This problem is being examined.

##### Glove Box Facilities for Transport Property Equipment

A preliminary schedule of work has been outlined for the installation of the two inert atmosphere glove boxes required for transport property measurements on unirradiated material. These boxes will contain the existing linear heat flow thermal conductivity apparatus in one box, and two Centorr high temperature furnaces (the thermal diffusivity and electrical resistivity furnaces) in the other. Design and fabrication work on this equipment is in progress.



## V. PUBLICATIONS

1. "Melting Behavior of (U, Pu) Monocarbides," J. G. Reavis, K. A. Johnson, and J. A. Leary, Plutonium 1970 and Other Actinides, edited by W. N. Miner (1970), pp. 791-798.
2. "Differential Thermal Analysis Observations of U-Pu Dicarbides," J. G. Reavis and J. A. Leary, Plutonium 1970 and Other Actinides, edited by W. N. Miner (1970), pp. 809-815.
3. "The Phase Equilibria and Thermal Expansion of the Carbon Saturated Plutonium Carbides," J. L. Green and J. A. Leary, Journal of Applied Physics, in press.
4. "Thermodynamic Properties of the Plutonium-Carbon System," G. M. Campbell, R. A. Kent, and J. A. Leary, Plutonium 1970 and Other Actinides, edited by W. N. Miner (1970), pp. 781-790.
5. "The Thermal Diffusivity of Heterogeneous Materials," J. F. Kerrisk, presented at the Tenth Thermal Conductivity Conference, Newton, Mass. (Sept. 1970)
6. "Thermal Diffusivity and Laser Beam Uniformity," K. W. R. Johnson and J. F. Kerrisk, presented at the Tenth Thermal Conductivity Conference, Newton, Mass. (Sept. 1970)

## VI. REFERENCES

1. Los Alamos Scientific Laboratory, "Quarterly Status Report on the Advanced Plutonium Fuels Program, April 1 to June 30, 1969 and Third Annual Report, FY 1969," LA-4284-MS, October, 1969, p. 85.
2. R. L. Cubitt, G. L. Ragan, D. C. Kirkpatrick, "Thermal Irradiation of Liquid Plutonium-Alloy Fuels," Los Alamos Scientific Laboratory Report No. LA-3832, June, 1968.
3. E. A. Aitken and S. K. Evans, U.S.A.E.C. Report GEAP-5672 (1968).
4. W. L. Lyon and W. E. Baily, U.S.A.E.C. Report GEAP-4878 (1965).
5. "Quarterly Status Report on the Advanced Plutonium Fuels Program, April 1 to June 30, 1968 and Second Annual Report FY 1968," Los Alamos Scientific Laboratory Report LA-3993-MS, (1968), p. 38.
6. "Quarterly Status Report on the Advanced Plutonium Fuels Program, April 1 to June 30, 1970 and the Fourth Annual Report, FY 1970," Los Alamos Scientific Laboratory Report LA-4494-MS, (1970), pp. 29-36.

7. H. K. Clark and J. L. Hoard, J. Am. Chem. Soc., 65, (1943), pp. 2115-2119.
8. J. J. Koulmann and R. Perol, C. R. Acad. Sci., Paris, Ser. A, B (1968), 267B (1), pp. 15-18.
9. A. H. Silver and P. J. Bray, J. Chem. Phys., 31, (1959) pp. 247-253.
10. G. A. Meerson and G. V. Samsonov, Zavodskaya Lab., 16, (1950), pp. 1423-1428.
11. S. Kitahara and T. Atoda, Rikagaku Kenkyusho Hokoku 34, (1958), pp. 339-343.
12. U.S.A.E.C. Report, KAPL-M-CWK-2, (1960).
13. YA. P. Gokhshtein and S. V. Pankrateva, Zavodskaya Lab., 36, (1970), pp. 274-275.
14. *Ibid.* p. 1
15. U.S.A.E.C. Report, ORNL-4560, (1970), pp. 143-162.
16. R. A. Kent, "Mass Spectrometric Studies of Plutonium Compounds at High Temperatures v. the Plutonium-Carbon System," presented at the International Conference on Mass Spectroscopy, Kyoto, Japan, (Sept. 1969).
17. "Quarterly Status Report on the Advanced Plutonium Fuels Program, April 1 to June 30, 1970, and Fourth Annual Report, FY 1970," Los Alamos Scientific Laboratory Report LA-4494-MS (1970), p. 38.
18. G. M. Campbell, R. A. Kent and J. A. Leary, "Thermodynamic Properties of the Plutonium-Carbon System," presented at the Fourth International Conference on Plutonium and Other Actinides, Santa Fe, New Mexico (Oct. 1970).
19. W. M. Olson and R. N. R. Mulford, "Thermodynamics of Nuclear Materials," IAEA, Vienna, (1968) p. 467.
20. P. S. Harris, B. A. Phillips, M. H. Rand, and M. Tetenbaum, UKAEA Report AERE-R 5353 (1967).
21. J. E. Battles, W. A. Shinn, P. E. Blackburn, and R. K. Edwards, High Temp. Sci., 2, 80, (1970).
22. J. P. Marcon, J. Inorg. Nucl. Chem., 32, 2581 (1970).
23. R. A. Kent, High Temp. Sci., 1, 169 (1969)
24. J. G. Reavis and J. A. Leary, "Thermal Analysis Observations of the (U, Pu)C<sub>2</sub> System,"

presented at the Fourth International Conference on Plutonium and Other Actinides, Santa Fe, New Mexico, (Oct. 1970).

25. M. H. Rand, Atomic Energy Review, 4, Special Issue 1, (1966).
26. JANAF Thermochemical Tables, The Dow Chemical Co., Midland, Michigan, 1965 and Supplement.
27. M. H. Rand, "A Thermochemical Assessment of the Plutonium-Carbon System," presented at a panel meeting, IAEA, Vienna, (Sept. 1968).
28. G. K. Johnson, Argonne National Laboratory, private communication, 1970.
29. E. K. Storms, The Refractory Carbides, Academic Press, New York, 1967.
30. R. A. Kent, and J. A. Leary, High Temperature Science, 1, 176 (1969).
31. D. E. Stellrecht, M. S. Farkas, and D. P. Moak, "Compressive Creep of Uranium Carbides," J. Am. Ceram. Soc., 51, (8), (1958), pp. 455-58.
32. C. H. deNovion, B. Amice, A. Groff, Y. Guerin, and A. Padel, "Mechanical Properties of Uranium and Plutonium-Based Ceramics," Plutonium 1970 and Other Actinides, Part 1, edited by W. N. Miner, Proceedings of the Fourth International Conference on Plutonium and Other Actinides, Santa Fe, New Mexico, (Oct. 1970), pp. 509-517.
33. R. R. Vandervoort, W. L. Barmore, and C. F. Cline, "Compressive Creep of Polycrystalline Uranium Mononitride in Nitrogen," Trans. Met. Soc. A.I.M.E., 242, (1968) pp. 1466-1467.
34. A. M. Killey, E. King, and H. J. Hedger, "Creep of U and (U, Pu) Monocarbides in Compression," AERE-R 5486, Presented at the Fourth International Conference on Plutonium and Other Actinides, Santa Fe, New Mexico, (Oct. 1970).
35. H. J. Hedger, personal communication, October 7, 1970.

PROJECT 472

ANALYTICAL STANDARDS FOR FAST BREEDER REACTOR OXIDE FUEL

Person in Charge: R. D. Baker  
Principal Investigator: C. F. Metz

I. INTRODUCTION

Necessary to the development of the high quality fuel and cladding required by the LMFBR/FFTF program are reliable analytical methods for the chemical characterization of the raw materials and the manufactured fuel and for the examination of irradiated fuel.

The more immediate objectives of this project are (1) the evaluation of existing analytical methods used by potential producers of FFTF fuel, (2) upgrading those methods found to be inadequate and the development of new methods as required by additional specifications, (3) the preparation of standardized calibration materials required by various analytical methods used for specification analyses and the distribution of these materials to producers of FFTF fuel, (4) the preparation of a manual of analytical methods for FFTF fuel, (5) development of a statistically designed quality assurance program for the chemical characterization of FFTF fuel as required by commensurate specifications, and (6) provide aid, as requested, for the prequalification programs of potential FFTF fuel producers.

These more immediate objectives will be continued, as required by the development of new fuel compositions for LMFBR demonstration plants and the new or additional chemical specifications that will be necessary for their characterization.

Additional objectives of this program involve studies of irradiated fuel including (1) the development of fuel burnup measurement methods based on conventional and spark source mass spectrometric determinations of

actinide and fission product isotopes, (2) the development of faster fuel burnup measurement methods based on chemical analysis techniques for use for larger routine sample loads, (3) the applications of burnup methods correlated with other measurement techniques including microprobe and metallographic examinations to assess the irradiation behavior of LMFBR/FFTF fuels, (4) the measurement of fission yields, and cross sections, as necessary, to ensure highly reliable burnup methods, (5) the development of analytical methods for gases including hot cell techniques for the evaluation of their effects on cladding stability, (6) the development of mass spectrometer methods, including hot cell techniques, for studies of the gas retention properties of fuels as a function of temperature-time cycling, and (7) the application of ion emission microanalysis to elucidate migration mechanisms in irradiated fuels.

II. FFTF ANALYTICAL CHEMISTRY PROGRAM  
(J. E. Rein, C. F. Metz, G. M. Matlack,  
R. T. Phelps, G. R. Waterbury)

A LASL document entitled "Program for the Qualification of Analytical Chemistry Laboratories for FFTF Fuel Analysis", written for possible adoption as an RDT Standard, was acceptable to WADCO following one minor technical change. This document prescribes the course of action by which analytical laboratories establish their technical competence for the chemical characterization of FFTF fuel and also provides a quality control program for the continual evaluation of the analytical data obtained during periods of fuel production in the production plants and at WADCO. To implement the proposed RDT

Standard Program, a detailed plan was developed, as described in the LASL Report CMB-1-908, July 10, 1970, for the LASL effort in preparing calibration materials and quality control samples, and in the establishment and surveillance of the operation quality control program. Uranium and plutonium oxides for the matrices of the calibration materials and the quality control samples were chemically characterized at WADCO and more extensively at LASL, and were found to be adequate. These materials have been shipped from WADCO for the extensive preparation of the various blends as outlined in LASL Report CMB-1-908.

Preparation of a comprehensive manual of analytical methods for the FFTF fuel characterization is more than half completed, and a strong effort is being made to complete the manual during the next quarter. Included are methods that have been developed at LASL and other laboratories and have been proven by statistical evaluation of test-sample results, such as those published in LA Report No. 4407, "LMFBR/FFTF Fuel Development Analytical Chemistry Program, (Phase II)". The use of the calibration materials and other aspects of the LASL quality assurance program are detailed in these methods to assist in placing the analytical laboratories of the production facilities and WADCO on a common basis, and to ensure the high-quality analytical effort required for the production of successful fuel.

Modifications are being made to the laboratories which will house the two mass spectrometers scheduled for delivery next quarter. One of the instruments will be used on burnup studies, and the other mainly on fission gas analyses with some work on gas retention problems. The modifications are more than half completed, and the laboratories should be in readiness by the time the mass spectrometers are received.

### III. INVESTIGATION OF METHODS

An important part of the analytical chemistry program is the investigation and improvement of analytical methods, and development of new methods. The following analyses of sintered (U, Pu)O<sub>2</sub> for various specifications were investigated.

#### 1. Determination of S (G. C. Swanson, T. K. Marshall, G. R. Waterbury)

Testing was started of a provisional spectrophotometric method for measuring S, one of the more recent additions to the FFTF fuel specifications. In this method, the S in solutions of FFTF fuel and UO<sub>2</sub> and PuO<sub>2</sub> materials is reduced in boiling HI - H<sub>2</sub>PO<sub>3</sub> to H<sub>2</sub>S which is swept with Ar into a Zn(C<sub>2</sub>H<sub>3</sub>O<sub>2</sub>)<sub>2</sub> solution. The resulting ZnS is reacted with FeCl<sub>3</sub>, HCl, and p-phenylenediamine to form Lauth's Violet. The amount of S is calculated from the absorbance of the Lauth's Violet at 595 nm using a standard curve prepared from data obtained by analyzing known amounts of K<sub>2</sub>SO<sub>4</sub>.

Initial tests show that the absorbance is a non-linear function of the S content, and that the recovery of S is slightly dependent upon the total concentration of metal ions in the solution from which the H<sub>2</sub>S is volatilized. Test samples prepared from U metal and K<sub>2</sub>SO<sub>4</sub> are being analyzed repeatedly to obtain data for a statistical evaluation of the precision and accuracy of the method for U materials. The equipment will then be installed in gloveboxes for tests with Pu-containing samples.

#### 2. Determination of Dy, Eu, Gd, and Sm (H. M. Burnett, O. R. Simi)

Spectrographic measurement, following a TNOA (tri-n-octylamine) extraction separation,<sup>1,2</sup> is being applied to the determination of Dy, Eu, Gd, and Sm in (U, Pu)O<sub>2</sub>, UO<sub>2</sub>, and PuO<sub>2</sub> materials. As the specifications limit the total concentration of these rare earths to 100 ppm, with a detection limit of 12.5 ppm for each element, a method covering the concentration range of 10 to 200 ppm is the goal of this work.

The U and Pu are extracted from a 0.2-g oxide sample, dissolved in 1.5M HNO<sub>3</sub>-6M HCl-.005 MHF, into 20% TNOA in xylene in the presence of 5 mg of H<sub>3</sub>BO<sub>3</sub>. The aqueous phase is concentrated by evaporation to dryness and dissolution of the residue in 1 ml of 1M HCl. A 50 μl aliquot is evaporated on a pair of Cu electrodes and analyzed by a copper-spark technique.

Initial tests on UO<sub>2</sub> materials showed that the microgram quantities of U that remained in the aqueous phase, B, and some organic residues from the extraction

were being transferred to the Cu electrodes in adequate amounts to cause reduction of the spectral line intensities and an increase in the spectral background. A third extraction of the U from the concentrated (1 ml) aqueous phase into TNOA-xylene, evaporation of the aqueous phase with methanol to remove B, and heating the residue with HNO<sub>3</sub> and then igniting it at 400°C to destroy the organic matter effectively eliminated these three residuals. Analyses of relatively pure test samples using the method with these modifications showed that the relative precision (1 σ) of the method was 5%.

Application of the modified method to prepared test samples containing the impurity elements for which maximum concentration limits were specified showed a bias of 60%. The majority of the impurity elements followed the rare earths through the separation, depressed the line intensities, and might have affected the intensity ratios of analytical to internal standard lines. Two ways were found to circumvent the effects of the impurity elements. The first was Cu spark excitation in an argon atmosphere instead of air. Although line intensities were reduced by the impurities, the intensity ratios were not changed as shown by coincident analytical curves (log-log plots of intensity ratios vs concentrations) obtained for calibration samples processed by this method with and without impurities. The precision was degraded to 15% relative standard deviation, however, when impurities were present. The second approach was d.-c. arc excitation of the rare earths in a Y<sub>2</sub>O<sub>3</sub> matrix. An amount of Y, equivalent to 50 mg of Y<sub>2</sub>O<sub>3</sub>, in HNO<sub>3</sub> solution was added to the final residue. After evaporation and ignition to the oxide, the sample was prepared by mixing with graphite and homogenizing, and then excited by a high current d.-c. arc in an Ar-O<sub>2</sub> atmosphere. Satisfactory analytical curves were obtained for the range 10 to 200 ppm using Y as an internal standard. The precision, based on limited data, was estimated to be 20% relative standard deviation.

Work is now in progress to evaluate the method with Pu and mixed U-Pu samples.

### 3. Determination of O/M Atom Ratios (G. C. Swanson, G. R. Waterbury)

Investigation of the many problems involved in the measurement of O/M atom ratios has continued, following the development of a recommended thermogravimetric method, because of the importance of this chemical property on the behavior of oxide reactor fuels. The recommended method included an oxidation of the oxide fuel in air at 1000°C to a hyperstoichiometric dioxide followed by a reduction in He-8% H<sub>2</sub> at 1000°C to the exactly stoichiometric dioxide. The O/M ratio was calculated from the initial and final weights. Impurities having oxidation-reduction behaviors different than those of the matrix oxides would cause errors in the measured O/M ratios. For this reason, the effects on the recommended method of impurities, either commonly found in sintered oxide fuels or included in the tentative FFTF fuel specifications, were determined using test samples prepared from, first, a mechanical mixture of unsintered, high-purity, U<sub>3</sub>O<sub>8</sub> and PuO<sub>2</sub>, and second, finely ground, sintered (U<sub>0.75</sub>Pu<sub>0.25</sub>)O<sub>2</sub> pellets. It was found that Ni, Ni<sub>2</sub>O<sub>3</sub>, Fe, and Al<sub>2</sub>O<sub>3</sub>, at levels ranging from 375 to 2000 ppm as the metal, did not change the measured O/M ratio of either the sintered or unsintered oxides by as much as ± 0.003 (Table 472-I), but Ca, CaO, FeO<sub>3</sub>, Al, and C, at metal or elemental concentrations of 420 to 1100 ppm, caused errors of ± 0.004 to -0.026.

Combinations of Al, Fe, Cr, Ni, Si, and Ti and combinations of their oxides at a total metal concentration of 1000 ppm caused much larger effects especially if the Al content was high. Addition of Na and S as Na<sub>2</sub>SO<sub>4</sub> corroded the fused silica boat and furnace tube, and the results obtained were not considered reliable and were

Table 472-I  
Effects of Selected Impurities on the Thermogravimetric Determination of O/M Ratio

Element	Form	Concentration <sup>a</sup>		Effect on O/M Ratio <sup>b</sup>	
		Unsintered	Sintered	Unsintered	Sintered
Ca	metal	1025	1100	-0.006	-0.005
	CaO	420	570	+0.004	+0.006
Ni	metal	1050	2000	-0.003	-0.003
	Ni <sub>2</sub> O <sub>3</sub>	535	890	+0.003	-0.002
Fe	metal	965	775	-0.003	0.000
	Fe <sub>2</sub> O <sub>3</sub>	595	615	+0.004	+0.006
Al	metal	995	1035	-0.026	-0.025
	Al <sub>2</sub> O <sub>3</sub>	375	565	0.000	-0.001
C	elemental	965	855	+0.013	+0.014
Al, Cr, Fe Ni, Si, Ti	metal	300 to 600 ppm each		-0.009 to -0.032	-0.006
	oxides	50 to 150 ppm each		+0.003 to -0.001	+0.005 to +0.003

<sup>a</sup> ppm of the element whether added as metal, oxide, or compound.

<sup>b</sup> Average of duplicate determinations.

not included in the table.

The reference oxide used in these studies was an unsintered, mechanical blend of  $U_3O_8$  and  $PuO_2$  prepared with known  $O_2$  content from the high-purity metals. Such a mixture might react differently in the oxidation-reduction cycle of the analytical method than a  $(U_{0.75}Pu_{0.25})O_2$  solid solution. Preparation of a solid solution oxide reference, therefore, is being attempted by mixing the HCl solutions of accurately weighed samples of U and Pu metals, each containing < 100 ppm detected impurities, in the correct proportions, evaporating the solution with  $HClO_4$ , and igniting the residue in  $He-O_2$  at a final temperature of  $1000^\circ C$ . The recommended thermogravimetric method will be tested using this mixed oxide reference when preparation is completed.

#### 4. Determination of $Cl^-$ and $F^-$

(T. K. Marshall, N. L. Koski, G. R. Waterbury)

Measurement of the concentrations of  $Cl^-$  and  $F^-$  in  $UO_2$ ,  $PuO_2$ , and  $(U,Pu)O_2$  are especially important because of the gross effects of the halides on the corrosion rates of stainless-steel cladding materials. Reliable methods were developed and tested previously for measuring  $F^-$  concentrations as low as  $1 \mu g/g$  and  $Cl^-$  concentrations down to  $10 \mu g/g$ , but a more sensitive measurement of  $Cl^-$  and less time-consuming methods were desired. In the original methods, separate samples were used. The  $F^-$  was separated pyrohydrolytically by passing steam over the oxide sample at  $1000^\circ C$  in an all-Ni apparatus, and  $Cl^-$  was separated by a pyrohydrolysis at  $1000^\circ C$  using moist Ar as the reactant in a fused-silica system. The  $F^-$  was measured in the condensate with a fluoride ion specific electrode, and the  $Cl^-$  was measured spectrophotometrically by reacting it with  $Hg(CNS)$  and  $Fe^{+3}$  to form the highly colored  $Fe(CNS)_3$ .

A combination of the two methods is being tested to improve the sensitivity of the  $Cl^-$  determination and to reduce the analysis time required. The  $Cl^-$  and  $F^-$  are separated simultaneously from one sample by pyrohydrolysis at  $1000^\circ C$  using Ni boats, a fused-silica furnace tube, and moist Ar as the reactant gas. The HCl and HF generated are collected in 7 ml of distilled water, as compared to 20 ml of weak base previously, in order to increase the

sensitivity. The  $F^-$  is measured in a small aliquot of the distillate with the  $F^-$  ion specific electrode, and the  $Cl^-$  is measured spectrophotometrically as before except the final volume is 10 ml as compared to 25 ml previously. At this time, a new  $F^-$  ion specific electrode is being calibrated for this application, and pyrohydrolysis conditions are being investigated to ensure quantitative recovery of each halide.

#### 5. Determination of $H_2O$ and Gases Evolved

(D. E. Vance, M. E. Smith, G. R. Waterbury)

Internal pressures in sealed reactor fuel capsules are dependent to a significant extent on the quantities of gases, including  $H_2O$  vapor, evolved from the fuel at operating temperatures. In the present methods, the amount of  $H_2O$  vapor released at  $800^\circ C$  is measured separately from the other gases evolved at  $1600^\circ C$ . A fuel pellet is heated in a fused-silica furnace tube at  $800^\circ C$ , the evolved  $H_2O$  is swept by Ar to a moisture monitor, and the monitor signal is integrated to obtain a quantitative measure of the  $H_2O$ . As some controversy exists concerning the optimum temperature for quantitative release of  $H_2O$ , the quantities evolved from each of seven pellets at several temperatures between 200 and  $950^\circ C$  were measured (Table 472-II). All of the water was evolved from each pellet at a temperature of  $400^\circ C$  or lower as indicated in the table. Pellets AUA-20-1 and -2 had been exposed to 50% relative humidity for approximately 1 yr prior to these tests, and the  $H_2O$  content was greater than  $50 \mu g/g$ . The  $H_2O$  was evolved in two distinct peaks, one starting at a temperature of  $200^\circ C$  and the other starting at a temperature of  $280^\circ C$  for pellet

Table 472-II  
Moisture Evolved from Pellets at Various Temperatures

Pellet Designation	Water Evolved, $\mu g/g$ , at					
	$200^\circ C$	$280^\circ C$	$300^\circ C$	$360^\circ C$	$380^\circ C$	$400^\circ C$
AUA-20-1	a	a	0.0	0.0	0.0	0.0
-2	b	b	a	a	0.0	0.0
-3	b	b	b	b	b	2.5
-4	b	b	b	b	b	2.2
-5	1.5	0.0	0.0	0.0	1.0	0.0
-6	0.7	0.0	1.1	0.0	0.0	0.0
AUA-21-7	21.6	0.0	0.0	0.0	0.0	0.0

<sup>a</sup>Quantity of  $H_2O$  was greater than  $50 \mu g/g$

<sup>b</sup>Starting temperature was  $300^\circ C$  for AUA-20-2 and  $400^\circ C$  for AUA-20-3 and -4.

AUA-20-1, and starting at 300°C and at 360°C for pellet AUA-20-2. The temperature was held at intermediate levels until H<sub>2</sub>O evolution at that temperature was complete as shown by the trace on the strip chart recorder of the moisture monitor. The occurrence of two separate H<sub>2</sub>O evolution peaks for some pellets indicated that the H<sub>2</sub>O might be present in the fuel pellets in two different states. From these results, the indicated minimum temperature for this analysis was 400°C.

In order to show the effects of the environment on the adsorption of H<sub>2</sub>O by the pellets during storage, three additional fuel pellets were dried at 600°C for 10 h in a stream of He, and then treated as follows: (1) pellet AUA-20-1 was placed in a sealed jar over H<sub>2</sub>O for 24 h, (2) pellet AUA-20-2 was stored in a small desiccator with anhydrous Mg(ClO<sub>4</sub>)<sub>2</sub> for 28 h, and (3) pellet AUA-20-3 was stored in a desiccator for 24 h and then exposed to the drybox atmosphere at approximately 40% relative humidity for 24 h. The quantities of H<sub>2</sub>O evolved at each of several temperatures were then measured (Table 472-III). The results showed that the pellets adsorb H<sub>2</sub>O if exposed to moist air and the amount adsorbed is dependent upon the relative humidity. The adsorbed water is evolved quantitatively at 200°C. It was concluded that a pretreatment of the pellets by drying at 110°C in an oven for 2 h and storage in a desiccator until analyzed would remove surface adsorbed H<sub>2</sub>O. This treatment could be duplicated easily in any laboratory, and each laboratory could thus have a common starting point in the analyses.

Volatiles other than H<sub>2</sub>O in reactor fuel pellets are determined by a vacuum extraction method at 1600°C. The sample is heated in a W crucible by induction, evolved H<sub>2</sub>O vapor is removed by anhydrous Mg(ClO<sub>4</sub>)<sub>2</sub>, and the remaining gases are collected by a Teoppler pump and measured. The large amount of H<sub>2</sub>O in the evolved gases

raised suspicions about the reduction of H<sub>2</sub>O by the W crucible at elevated temperatures. For this reason, the H<sub>2</sub>O-W reaction was studied by determining with a mass spectrometer the H<sub>2</sub> in the reaction products formed when moist Ar was heated with W powder. A definite reaction was observed at 400°C in 20 min, and measurable quantities of H<sub>2</sub> were formed. At 350°C, no reaction occurred within 45 min. These results indicate that reactions between evolved H<sub>2</sub>O and the W crucible may produce a very small amount of the observed H<sub>2</sub>. A W crucible should not be recommended, however, in the method for measuring H<sub>2</sub>O. A much larger quantity of H<sub>2</sub> probably comes from the H<sub>2</sub> adsorbed by the pellets from the H<sub>2</sub>-rich sintering furnace atmosphere. Cooling of the reduced pellets in an inert atmosphere greatly reduced the H<sub>2</sub> content of the gases evolved at 1600°C.<sup>3</sup>

A final report describing the method for measuring H<sub>2</sub>O is now in preparation.

#### 6. Determination of Metal Impurities

(J. V. Pena, W. M. Myers, C. J. Martell, C. B. Collier, R. T. Phelps)

Control of metal impurities in sintered (U, Pu)O<sub>2</sub> fuel pellets is dependent upon reliable spectrographic analyses of the UO<sub>2</sub> and PuO<sub>2</sub> raw materials as well as the pellets. Changes made recently in the FFTF Analytical Chemistry Program (LA Document CMB-1-908, 1970) have required further study of the spectrographic methods and modifications to include measurement of Be, Co, K, Li, and Ta, thereby increasing the number of impurities determined to 25 each at a concentration ranging between 25% and 100% of the specification value (Table 472-IV). The quality control samples containing all of

Table 472-IV  
Specification Values of General Impurity Elements in  
UO<sub>2</sub>, PuO<sub>2</sub> and (U, 75Pu, 25)O<sub>2</sub>

Element	Concentration, ppm, of each impurity
Al, Fe, Na, Ni, V	500
Si, Ta	400
Ca, Cr	250
Cu, K, Ti, Zn	200
Ag, Mg, Mn, Mo, Pb, Sn, W	100
B, Be, Cd	20
Co, Li	10

Table 472-III

Moisture Evolved from Pellets at Various Temperatures

Pellet Designation	Water Evolved, μg/g. at		
	200°C	400°C	500°C
AUA-20-1	3.4	0.0	0.0
-2	0.0	0.0	0.0
-3	0.7	0.0	0.0

the impurities at the concentrations shown are quite impure (3000 ppm of impurity elements), and may present problems not encountered when analyzing the Phase II fuel pellets containing < 300 ppm of total detected impurities. For the further studies of the methods, calibration materials were prepared with  $U_3O_8$ ,  $PuO_2$ , or  $(U_{0.75}Pu_{0.25})O_2$  matrices, and each contained all 25 impurity elements at concentrations graduated in direct proportion to the specification values (Table 472-IV). A  $U_3O_8$  matrix was used in the calibration material in place of  $UO_2$  because the analysis of  $UO_2$  includes conversion to  $U_3O_8$ . Based upon these studies, modifications in the methods were made to meet the new requirements for each material.

#### $UO_2$ Methods

Two methods are now used in analyzing  $UO_2$  (Table 472-V). The majority of the 25 impurity elements is determined using 4%  $Ga_2O_3$  as the carrier and added Co as the internal standard. The wide spectral coverage of the spectrograph (ARL, 2m, grating spectrograph with two cameras each covering 2000Å of spectrum) for these analyses allows determination of K, Li, and Na along with other impurities. A slight modification has been a lowering of the arcing current, primarily, to lower the intensity signal of K and Na. High detection sensitivity, 0.5 ppm, needed only for Li, can be attained at the lower current. The refractory elements and Co are determined with AgCl carrier and Pd internal standard as reported

Table 472-V  
Carrier-Distillation Methods Used for Analysis of  $UO_2$ ,  $PuO_2$  and  $(U_{0.75}Pu_{0.25})O_2$

Sample	Carrier	Arc Atmos.	Charge, mg.	Int. Std.	Impurity
$UO_2$	4% $Ga_2O_3$ + 2.4% C	Air	100	200 ppm Co	Ag, Al, B, Be, Ca, Cd, Cr, Cu, Fe, Li, K, Mg, Mn, Na, Ni, Pb, Si, Sn, Zn
$UO_2$	15% AgCl	$O_2$	130	500 ppm Pd	Co, Mo, Ta, Ti, V, W
$PuO_2$	4% $Ga_2O_3$	$O_2$	100	500 ppm Co	Ag, Al, B, Be, Ca, Cd, Cr, Cu, Fe, Mg, Mn, Mo, Ni, Pb, Si, Sn, V, Zn
$PuO_2$	4% $Ga_2O_3$	$O_2$	100		Li, K, Na
$PuO_2$	50% AgCl	$O_2$	50	500 ppm Pd	W, Mo, V
$PuO_2$	15% AgCl	$O_2$	120	500 ppm Pd	Co, Mo, Ta, Ti, V
$(U_{0.75}Pu_{0.25})O_2$	5.4% $Ga_2O_3$	$O_2$	100	800 ppm Co	Ag, Al, B, Be, Ca, Cd, Cr, Cu, Fe, Mg, Mn, Ni, Pb, Si, Sn, Zn
$(U_{0.75}Pu_{0.25})O_2$	5.4% $Ga_2O_3$	$O_2$	100		Li, K, Na
$(U_{0.75}Pu_{0.25})O_2$	40% AgCl	Air	25	500 ppm Pd	W, Mo, V
$(U_{0.75}Pu_{0.25})O_2$	15% AgCl	$O_2$	120	500 ppm Pd	Co, Ta, Ti

previously.<sup>4</sup>

The concentrations of several impurities, including Ca, Cd, Li, K, and Na, are evaluated either visually or photometrically from the spectrograms, but without use of an internal standard. Generally, the precision of results obtained by visual comparison is 50% relative standard deviation. Using an internal standard when applicable improves the precision to 20% relative standard deviation.

#### $PuO_2$ Methods

The determination of impurities in  $PuO_2$  now requires four methods, two by using 4%  $Ga_2O_3$  carrier and two using AgCl carrier (Table 472-V). Two methods using 4%  $Ga_2O_3$  carrier are required because the spectral coverage of the spectrograph (Jarrell Ash, Ebert mounting, with 30 in. camera) is not adequate to include the K lines at wavelengths of 7665Å and 7699Å with the lines of the other impurity elements. By determining Li, Na, and K separately, the detection sensitivity for Li is 0.25 ppm as compared to 1 ppm when included with the measurements of other impurities. Two AgCl carrier methods, using different concentrations of carrier and electrode-charge sizes, are needed to obtain suitable detection limits for Ta, and W. Internal standards are used in the determinations of Al, Cr, Fe, Mn, Ni, Si, Ta, and W, and the precision is 20 relative percent. Concentrations of the other impurities are evaluated either visually, with 50% relative standard deviation, or photometrically from the spectrograms.

#### $(U_{0.75}Pu_{0.25})O_2$ Methods

Four methods, similar to those used to analyze  $PuO_2$ , are required (Table 472-V) for  $(U_{0.75}Pu_{0.25})O_2$  which offers the greatest possibility of spectral interference because both U and Pu are present. Two methods using  $Ga_2O_3$  carrier are required to cover the spectral range of the impurity element lines including K. Two AgCl carrier methods are needed because W is determined more reliably in this matrix by arcing the sample in air, but arcing in  $O_2$  is preferred for measurement of Co, Ta, and Ti.

The elements determined in  $(U_{0.75}Pu_{0.25})O_2$  by use of the internal standards are Al, Cr, Fe, Mn, Ni,



Si, Ta and W, and wider application of the internal standard technique is being studied. The other elements are determined either by visual comparison or by photometric measurement of the line intensities of the spectrograms. Photometric measurement provides better reliability because the measurement is less subjective and all calibration data may be examined rather than just the data that bracket the sample result. Visual comparison is faster and often 50% relative precision ( $1\sigma$ ) obtained is adequate.

#### 7. Determination of P

(R. G. Bryan, T. Romero, G. R. Waterbury)

Measurement of P in  $\text{PuO}_2$ ,  $\text{UO}_2$ , and  $(\text{U}, \text{Pu})\text{O}_2$  at concentrations between 10 and 200  $\mu\text{g/g}$  is required to ensure that the specifications regarding this impurity have been met. A method for determining P in Pu metal is being adapted for this purpose. The oxide sample, following dissolution in  $\text{HNO}_3$ -HF or in HCl, is fumed to incipient dryness with  $\text{H}_2\text{SO}_4$  and HF to volatilize Si impurity, and the residue is dissolved in  $(\text{NH}_4)_2\text{MoO}_4$  to form phosphomolybdic acid which is extracted into n-butanol. Washing the extract with aqueous  $\text{SnCl}_2$  reduces the extracted phosphomolybdic acid, and the absorbance of the intense blue color of the reduced phosphomolybdic acid is measured spectrophotometrically at 725 nm. The P content is calculated from the absorbance and the average absorbance/ $\mu\text{g}$  P obtained for samples containing known amounts of P.

Preliminary data indicate that between 0.5 and 10  $\mu\text{g}$  of P in a 50 mg sample can be quantitatively extracted and measured spectrophotometrically with a relative precision ( $1\sigma$ ) of 3%. Repeated measurements of P added to solutions containing U and Pu are being made to determine the reliability of the method for analyzing the oxide samples of interest to the program.

#### IV. REFERENCES

1. R. Ko, BNWL-SA 2450A, 1969.
2. PNL Manual BNWL-1024, Method No. 20.9, 1970.
3. W. H. Pechin and R. A. Bradley, ORNL-4520, Part III, p. 20, 1970.
4. Quarterly Status Report on Advanced Plutonium Fuels Program, LA-4494-MS, p. 94, 1970.

SPECIAL DISTRIBUTION

Atomic Energy Commission, Washington

Division of Research

D. K. Stevens

Division of Naval Reactors

R. H. Steele

Division of Reactor Development and Technology

G. W. Cunningham

D. E. Erb

Nicholas Grossman

W. H. Hannum (2)

K. E. Horton

J. R. Humphreys

R. E. Pahler

Sol Rosen

J. M. Simmons (2)

E. E. Sinclair

Bernard Singer

C. E. Weber

G. W. Wensch

M. J. Whitman

Division of Space Nuclear Systems

G. K. Dicker

F. C. Schwenk

Safeguards & Materials Management

J. M. Williams

Idaho Operations Office

DeWitt Moss

Ames Laboratory, ISU

O. N. Carlson

W. L. Larsen

M. Smutz

Argonne National Laboratory

A. Amorosi

R. Avery

F. G. Foote

Sherman Greenberg

J. H. Kittel

W. B. Loewenstein

P. G. Shewmon

Idaho Falls, Idaho

D. W. Cissel

Milton Levenson

R. C. Robertson

Atomics International

R. W. Dickinson, Director (2)

Liquid Metals Information Center

J. L. Ballif

Babcock & Wilcox

C. Baroch

J. H. MacMillan

Donald W. Douglas Laboratories

R. W. Andelin

General Electric Co., Cincinnati, Ohio

V. P. Calkins

General Electric Co., Sunnyvale, California

R. E. Skavdahl

Gulf General Atomic, Inc.

E. C. Creutz

Idaho Nuclear Corporation

W. C. Francis

IIT Research Institute

R. Van Tyne

Lawrence Radiation Laboratory

Leo Brewer

J. S. Kane

A. J. Rothman

LMFBR Program Office

D. K. Butler (Physics)

P. F. Gast

L. R. Kelman (Fuel & Materials)

J. M. McKee (Sodium Technology)

Mound Laboratory

R. G. Grove

NASA, Lewis Research Center

J. J. Lombardo

Naval Research Laboratory

L. E. Steele

Oak Ridge National Laboratory

G. M. Adamson

J. E. Cunningham

J. H. Frye, Jr.

C. J. McHargue

P. Patriarca

O. Sisman

M. S. Wechsler

J. R. Weir

Pacific Northwest Laboratory

F. W. Albaugh

E. A. Evans

V. J. Ruykauskas

W. R. Wykoff

FFTF Project

E. R. Astley

B. M. Johnson

D. W. Shannon (2)

**Battelle Memorial Institute**

D. L. Keller  
S. J. Paprocki

**Brookhaven National Laboratory**

D. H. Gurinsky  
C. Klamut

**Combustion Engineering, Inc.**

S. Christopher

**U. S. Department of Interior**

Bureau of Mines, Albany, Oregon

H. Kato

**United Nuclear Corporation**

A. Strasser

**Westinghouse, Advanced Research Division**

E. C. Bishop

**Australian Atomic Energy Commission**

J. L. Symonds